AD-A129 227 ON THE STRUCTURE OF AN UNDEREXPANDED RECTANGULAR JET (U) STANFORD UNIV CA JOINT INST OF AERONAUTICS AND ACOUSTICS A KROTHAPALLI ET AL. JUL 82 JIAA-TR-47 1/1

UNCLASSIFIED AFOSR-TR-83-0454 F49620-79-C-0189 F/G 20/4 NL

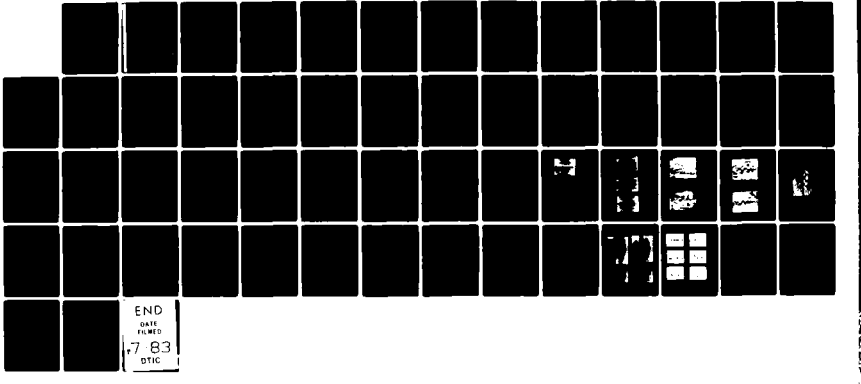

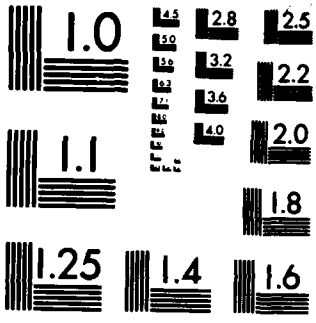

(6)

JOINT INSTITUTE FOR AERONAUTICS AND ACOUSTICS

NASA
National Aeronautics and
Space Administration
Ames Research Center

Stanford University

JIAA TR - 47

ON THE STRUCTURE OF AN UNDEREXPANDED RECTANGULAR JET

A. Krothapalli, Y. Hsia, D. Baganoff, and K. Karamcheti

STANFORD UNIVERSITY
Department of Aeronautics and Astronautics
Stanford, California 94305

JULY 1982

SECURITY CLASSIFICATION OF THIS PAGE (When Data Entered)

REPORT DOCUMENTATION PAGE		READ INSTRUCTIONS BEFORE COMPLETING FORM
1. REPORT NUMBER AFOSR-TR- 83-0454	2. GOVT ACCESSION NO. AD-A129	3. RECIPIENT'S CATALOG NUMBER 227
4. TITLE (and Subtitle) ON THE STRUCTURE OF AN UNDEREXPANDED RECTANGULAR JET		5. TYPE OF REPORT & PERIOD COVERED INTERIM
		6. PERFORMING ORG. REPORT NUMBER
7. AUTHOR(s) A KROTHAPALLI, D BAGANOFF, Y HSIA, K KARAMCHETI		8. CONTRACT OR GRANT NUMBER(s) F49620-79-C-0189
9. PERFORMING ORGANIZATION NAME AND ADDRESS STANFORD UNIVERSITY DEPT OF AERONAUTICS & ASTRONAUTICS STANFORD, CA 94305		10. PROGRAM ELEMENT, PROJECT, TASK AREA & WORK UNIT NUMBERS 61102F 2307/A1
11. CONTROLLING OFFICE NAME AND ADDRESS AIR FORCE OFFICE OF SCIENTIFIC RESEARCH/NA BOLLING AFB, DC 20332		12. REPORT DATE July 1982
		13. NUMBER OF PAGES 47
14. MONITORING AGENCY NAME & ADDRESS (if different from Controlling Office)		15. SECURITY CLASS. (of this report) Unclassified
		15a. DECLASSIFICATION/DOWNGRADING SCHEDULE

16. DISTRIBUTION STATEMENT (of this Report)

Approved for Public Release; Distribution Unlimited.

17. DISTRIBUTION STATEMENT (of the abstract entered in Block 20, if different from Report)

18. SUPPLEMENTARY NOTES

19. KEY WORDS (Continue on reverse side if necessary and identify by block number)

RETANGULAR JET
UNDEREXPANDED JET
TURBULENT JET STRUCTURE

20. ABSTRACT (Continue on reverse side if necessary and identify by block number)

An experimental investigation has been carried out on an underexpanded jet of air issuing from a converging rectangular nozzle of moderate aspect ratio. Schlieren pictures of the flow field along with hot-wire measurements in the jet were obtained at different pressure ratios. At the pressure ratio corresponding to the maximum screeching sound, Schlieren photographs show a very strong organized cylindrical wave pattern on either side of the jet, with their respective sources being located at the end of the third shock cell. Associated with this wave pattern is a large increase in

DD FORM 1 JAN 73 1473 EDITION OF 1 NOV 65 IS OBSOLETE

UNCLASSIFIED

SECURITY CLASSIFICATION OF THIS PAGE (When Data Entered)

the angle of spread of the jet. It is shown that the self excitation helps to induce large-scale vortical motions in the jet both in the plane containing the small dimension of the nozzle and in the plane containing the long dimension of the nozzle. However, the locations of these structures are different in the two planes. Nevertheless, the characteristic Strouhal number corresponding to these large-scale structures in both planes is the same and equal to 0.12. The influence of the self excitation on the mean velocities and rms intensities has also been investigated. For the full range of pressure ratios studied, similarity was found both in the mean velocity and rms intensity profiles in the two central planes beyond 80 widths downstream of the nozzle exit. However, the shapes of the similarity profiles are differnt in the two planes. For the downstream distances studied, complete axisymmetry (identical mean velocity profiles in both planes) was not found, which suggests it may persist for a large distance downstream of the nozzle exit.

JIAA TR-47

ON THE STRUCTURE OF AN UNDEREXPANDED RECTANGULAR JET

A. Krothapalli, Y. Hsia, D. Baganoff, and **K. Karamcheti**

The work presented here has been supported by the Air Force Office of Scientific Research under contract F49620-79-0189.

ABSTRACT

An experimental investigation ~~has been~~ was carried out on an underexpanded jet of air issuing from a converging rectangular nozzle of moderate aspect ratio. Schlieren pictures of the flow field along with hot-wire measurements in the jet were obtained at different pressure ratios. At the pressure ratio corresponding to the maximum screeching sound, Schlieren photographs show a very strong organized cylindrical wave pattern on either side of the jet, with their respective sources being located at the end of the third shock cell. Associated with this wave pattern is a large increase in the angle of spread of the jet. It is shown that the self excitation helps to induce large-scale vortical motions in the jet both in the plane containing the small dimension of the nozzle and in the plane containing the long dimension of the nozzle. However, the locations of these structures are different in the two planes. Nevertheless, the characteristic Strouhal number corresponding to these large-scale structures in both planes is the same and equal to 0.12. The influence of the self excitation on the mean velocities and rms intensities ~~has~~ was also ~~been~~ investigated.

For the full range of pressure ratios studied, similarity was found both in the mean velocity and rms intensity profiles in the two central planes beyond 80 widths downstream of the nozzle exit. However, the shapes of the similarity profiles are different in the two planes. For the downstream distances studied, complete axisymmetry (identical mean velocity profiles in both planes) was not found, which suggests it may persist for a large distance downstream of the nozzle exit.

ACKNOWLEGMENTS

We are indebted to many colleagues, visitors, and students of the Joint Institute for Aeronautics and Acoustics for helpful discussions and suggestions. We are also grateful to Professor D. G. Crighton and Professor C. K. Tam for their encouragement and suggestions during the course of this work.

TABLE OF CONTENTS

TABLE OF CONTENTS

LIST OF FIGURES

INTRODUCTION

The increased interest in V/STOL aircraft has caused a great deal of attention to be focussed on jet flows exiting from rectangular nozzles. In particular, the mixing characteristics of an underexpanded jet exiting from a converging rectangular nozzle of moderate aspect ratio is of great interest. As part of an ongoing program at Stanford to study the mixing characteristics of single and multiple rectangular jets both in free and confined configurations, a systematic investigation has been carried out on the structure of a jet issuing from a moderate aspect ratio rectangular nozzle at flow speeds ranging from low subsonic to supersonic. The detailed measurements of the mean and turbulent velocity components of an incompressible jet was reported by Krothapalli, et al., 1981. The effect of the exit Mach number on the overall flow field of a subsonic compressible jet was studied by Hsia et al., 1982a. This paper reports the results of a study of a supersonic rectangular jet (choked at the nozzle exit). In all these investigations the nozzle used was the same, thus providing an opportunity to assess systematically the various changes brought about by the varying flow conditions.

It is well known that the structure of a choked underexpanded jet displays different features to those of subsonic and ideally expanded or shock free supersonic jets. These features include discrete tones in the sound spectrum, known as screech tones, under certain conditions and an accelerated spreading of the jet with enhanced mixing. The jet "screech" phenomenon, an oscillatory condition common to underexpanded jet flows, is described by Powell 1953, as arising through a feed-back mechanism. A disturbance in the jet shear layer is convected downstream (assumed amplified in passing downstream) and strikes a cell boundary, scattering intense sound at that point. This sound propagates through the ambient medium in the upstream direction and interacts with the jet shear layer close to the jet exit, giving rise to a new downstream travelling disturbance that continues the cycle. The essential element of the cycle is the amplification of the downstream travelling disturbance. This process maintains itself mainly because the energy lost through scattered radiation and viscous effects is resupplied to the propagating disturbance by an instability of the flow. The detailed mechanism of screech tone generation is yet to be understood, although the general nature of the feedback loop, was treated by Powell who

developed a simple relation between tone frequency, cell size, and operating conditions. Under certain conditions, the concomitant sound production accelerates the spreading of the jet and enhances mixing. However, the conditions for the existence or absence of such a phenomenon cannot yet be predicted.

A considerable amount of experimental data is available in the literature to characterize the near sound field of a choked underexpanded jet (Powell 1953a, 1953b; Lassiter and Hubbard 1956; Davies and Oldfield 1962; Hammitt 1961; Harper-Bourne and Fisher 1973; Westley and Woolley 1973; Sherman, Glass and Dullep 1976; Krothapalli, Baganoff, Hsia and Karamcheti 1981, 1982). Most of the work reported in the literature has been associated with the flow field of an axisymmetric jet. Although the structure of a rectangular jet exhibits some features similar to that of an axisymmetric jet, there exists some important differences between the two flows. Some of these differences even make experimental study easier. For example, the nearly two-dimensional structure of the disturbances and their associated sound fields near the nozzle exit are easily identified in flow visualization pictures because of the long optical path length present. It is thus experimentally attractive to study the interaction between the sound field and the mean and turbulent components of the flow for the flow exiting from a rectangular nozzle.

The effect of acoustic feed back on the spreading and decay of an axisymmetric underexpanded jet was first studied by Glass 1968. However, his experimental study was limited to the measurement of gross properties of the flow because of his use of a pitot tube in the experiments. None of the works that followed presented information regarding the effects of screech tones or organized sound waves on the turbulent structure of the flow; in particular, none on the rectangular jet, the objective of the present paper. The detailed structure of the near sound field and its source for an underexpanded jet operating at maximum screech condition is to be given in a separate paper by Krothapalli et al., 1982.

The principal parameters or variables governing the flow of a free rectangular jet are the pressure ratio R (stagnation pressure/ambient pressure), Mach number M, and Reynolds number Re, the turbulence level of the flow at the exit of the nozzle, the conditions of the medium into which the jet is issuing, and the aspect ratio of the nozzle. In the present investigation the pressure ratio, R, was varied from 2 to 5.8. This interval corresponds to a Mach number range, based on fully expanded isentropic flow, of 1.05 to

1.8. The Reynolds number employed here is based on the width D of the nozzle (small dimension) and given by $Re = MaD/\nu$, where a and ν are the speed of sound and kinematic viscosity of the ambient medium respectively. This Reynolds number was varied from 7.2×10^4 to 1.0×10^5 in the experiment. A rectangular nozzle of aspect ratio 16.7 was studied. The inlet geometry of the nozzle was designed specifically to obtain a low turbulence level at the exit plane of the nozzle. The total-pressure profile at the exit plane of the nozzle was found to be quite flat.

APPARATUS, INSTRUMENTATION AND PROCEDURES

A high-pressure blow-down type air supply system was used to provide the air flow to a cylindrical settling chamber having dimensions of 1.75m long and 0.6m in diameter. The temperature in the settling chamber was maintained at a constant temperature, usually at room temperature, to an accuracy of about 0.5°C over the duration of each test. Before reaching the nozzle, the air was passed through an adapter, containing six screens set 5cm apart, to minimize disturbances at the nozzle inlet. The ratio of areas between the adapter and the nozzle exit was about 40. Two nozzle sizes were used in the study. The dimensions of the rectangular exit of the small nozzle used was 50mm long (L) by 3mm wide (D). The exit dimensions of the large nozzle were 50mm long and 5mm wide. The nozzle exit in each case was preceded by a 40mm long smooth rectangular channel (50mm $\times$ 3mm and 50mm $\times$ 5mm respectively). The 3mm nozzle used in the investigation, shown schematically in Figure 1, was a single central lobe of a multi-lobed nozzle employed in a related investigation. Most of the detailed measurements were made using the 3mm nozzle. The experiment made use of the same model and air supply system as that described by Krothapalli et al., 1981. A 7mm thick acoustic insulation was used to cover all exposed surfaces on the nozzle to minimize acoustic reflections from these surfaces.

A conventional Schlieren system was used for flow visualization purposes. The configuration employed was a single pass design, with the optical axis folded twice using two 25cm diameter, 3.05m focal length spherical mirrors. The light source employed was a stroboscopic flash unit having a 1.5μ sec flash duration. The stroboscopic feature was used for visual observations while single pulses were used for photographic records.

For downstream distances X/D less than 15, where the velocities are high and the flow contains shock waves, measurements were confined to the use of a pitot tube having an external diameter of about 0.46 mm and a diameter of the sensing tube of about 0.25 mm. Further downstream, in regions where the flow is known to be subsonic, hot-wire and/or hot-film anemometry was used.

All velocity measurements were made with a DISA 55 M10 constant - temperature anemometer in conjunction with a DISA 55 M25 linearizer. The hot wire used was a

DISA 55 P11 single normal platinum-coated tungsten wire with a 5μ m diameter and 1mm length. The hot film used was a DISA 55 R31, a wedge shaped 0.5μ m quartz coated nickel sensor with a 0.2mm width and 1mm length. The frequency response of the hot-wire electronics, in response to a square wave test with the probe placed in a high speed ($M = 0.8$) low turbulence jet, was approximately 40 KHz. The hot-wire and hot-film probes were calibrated using a low turbulence air jet regulated by a DISA 55 D90 calibration unit. The flow velocity, with correction for compressibility, is obtained as an analog voltage. The hot-wire output voltage was linearized for the velocity range 20m/sec to 280m/sec, with the output voltage E directly proportional to the velocity U($E = KU$, where K is a constant selected in conjunction with the linearizer gain control). Similarly, the hot film output voltage was linearized for the velocity range 20m/sec to 300m/sec. Despite the direct proportionality between the fluid velocity and the hot-wire voltage during calibration, the hot-wire fluctuation voltage e, in a turbulent compressible flow, will depend additionally upon fluctuations in the density and the total temperature (Horstmann and Rose, 1977). Lacking proper means to accurately correct velocity data for these fluctuations, rms values will be expressed in terms of $\tilde{e} = < e > /E$ (where $< e >$ denotes rms), which becomes equal to the turbulence intensity $< u > /U$ for low Mach numbers. The detailed calibration procedure used is given by Hsia et al., 1982b.

The signal from the linearizer was passed through a DISA type 55D31 digital voltmeter, a DISA type 55D35 rms unit, and a TSI model 1076 voltmeter to get the mean and rms values. Integration times with these instruments can be selected in discrete steps from 0.1 to 100 sec, and 10 sec was typically used. Spectral measurements were made using a Nicolet type 660B spectrum analyzer.

A cartesian coordinate system (X, Y, Z), defined in Figure 1, was employed with its origin located on the centerline of the jet. Hot-wire or hot-film traverses were made in the two central X, Y and X, Z planes at streamwise locations (X) from $40D$ to $160D$. In all the measurements, the sensor wire was oriented parallel to the Z axis. Mean velocity measurements were made across the entire jet in order to establish the symmetry of the flow about the central planes, however, only the data for each half plane will be presented.

The controlling parameter in this investigation was the stagnation pressure, p_o, which varied from 30psia to 85psia, and was maintained within an accuracy of $\pm$ 0.02psia. This

range corresponds to nozzle pressure ratios (stagnation pressure/ ambient pressure) varying from 2 to 5.8. The temperature in the settling chamber was maintained to within $\pm 0.5°C$ of the ambient temperature. Experiments were conducted for a number of pressure ratios using both nozzles, however, only a limited selection is presented here. The detailed hot-wire measurements were made using the 3mm nozzle and were limited to the three pressure ratios $R = 2.7$, $R = 3.8$, and $R = 5.4$.

RESULTS AND DISCUSSION

(a) Flow Visualization Study

Typical Schlieren pictures of the flow issuing from the 3mm nozzle for three different pressure ratios are shown in Figure 2. The knife edge was oriented parallel to the jet axis in these photographs. The Schlieren system was purposely adjusted to enhance the view of the wave structure in the outer region, rather than to show the details of the jet flow. Consequently, features such as shock cell structure are not seen clearly in these photographs. The long optical path associated with the rectangular geometry makes possible the viewing of wave systems that otherwise would not easily be seen. These pictures display the flow field from the nozzle exit to a down-stream location of about $30D$.

For pressure ratios $R > 1.9$, the flow beyond the nozzle exit is supersonic and results in the formation of a series of shock cells, as shown in Figure 2. The most striking observation for the three cases shown in the figure are the large changes in the angle of spread of the jet, the appearance of a very strong organized wave pattern, and the development of a Mach wave radiation pattern at the highest pressure ratio. For example, the total angle of spread of the jet is about 20° for both the lowest ($R = 2.7$) and the highest ($R = 5.4$) pressure ratios, while the total angle of spread is about 36° at the pressure ratio for maximum screech sound radiation ($R = 3.8$). Associated with the large spreading rate is an organized cylindrical double wave pattern which originates alternatively from the two sides of the jet. The center of the arcs formed by the sound waves on each side can be located and identified as the source for each wave system. This source is located approximately at the end of the third shock cell ($x/D = 7$). The picture seems to suggest that a principal wave length exists and that this wave length is the same for all directions of propagation of the wave. The second wave front seen in the figure introduces a second and much shorter characteristic length, which corresponds to a frequency much too high to record with ordinary detectors. A similar double wave pattern was observed by Powell 1953c, in his edge tone excitation of rectangular jets. For the pressure ratio $R = 5.4$, high frequency sound waves, emanating at an angle of about 45° to the direction of the stream, can be seen radiating from a region close to the jet exit. This apparent radiation

from the supersonic region of the jet was also observed by Lowson and Ollerhead 1968, in their experiments with ideally expanded axisymmetric jets, and they identified it with Mach-wave radiation. From the near field sound spectra, not shown here, discrete tones, known as screech tones, are observed in all three cases (Krothapalli et al., 1981). However, the simultaneous existence of an organized wave pattern with large spreading appears only in the range of pressure ratios from 3 to 4. On reviewing all the pictures taken in the study, an organized vortical structure appears to be identifiable in the shear layers on either side of the jet, and these grow in intensity as the pressure ratio approaches the value for maximum screech sound generation, which occurs here at $R = 3.8$.

To study the degree of two-dimensionality present in the flow, photographs were taken at right angles to the view shown in Figure 2. These results are presented in Figure 3 for the same conditions as those in Figure 2. Three shock cells can be identified in the photographs by the three bright lines in the jet, which are the shock waves at the end of each of the corresponding shock cells. For downstream distances x less than $10D$, organized lines are observed lying along the span of the jet. The spacing between them seems to increase with downstream distance. These lines suggest the presence of spanwise vorticies developing in the shear layers surrounding the cell structure (see Figure 2). Because of the concave nature of the shear layers, it is suggested by Morkovin 1981 that they may be Goertler vorticies (Schlichting 1980). These features are more clearly seen in Figure 4 to be discussed below. Very little spreading is observed for the lowest and highest pressure ratios, while at $R = 3.8$ the jet width first reduces at intermediate distances and then increases with downstream distance.

Figure 4 presents an example of the flow from the 5mm nozzle for conditions close to those for Figures 2b and 3b. In this case the aspect ratio of the nozzle is lower (10) than for the 3mm nozzle (16.7). On comparing the two flows in the plane containing the small dimension of the nozzle, one finds that a single wave pattern is present in Figure 4a, while a double wave pattern is present in Figure 2b. This feature was found in all of our tests and appeared to be associated with the larger aspect ratio of the 3mm nozzle. This may be consistent with the fact that when the aspect ratio is further reduced no double-wave pattern is seen, as in the case of circular jets (Thomson 1971). Because of the larger nozzle size, the shock cells can be seen more clearly in Figure 4a and evidence

of their large amplitude lateral oscillations is quite apparent in the photograph. Likewise, the source of the strong cylindrical waves seems to be located at the point where the third shock cell breaks up. The large scale vortical structures mentioned above can be seen more clearly in the picture and can be followed by their orderly dark patterns.

The photograph taken at right-angles to the view in Figure 4a is shown in Figure 4b. Three shock cells can be identified in the figure, and very little spreading of the jet occurs in this view, indicating the flow is fairly two dimensional within the region covered in the photograph. The organized spanwise disturbances or vorticies can be seen even more clearly in this photograph and can be followed for a considerable distance downstream.

It has been shown by Poldervaart et al. 1973, that the placement of a reflective surface near the exit of an underexpanded rectangular jet has an important effect on the flow. To further investigate this effect, several reflector geometries were used. Two typical geometries are shown in Figures 5 and 6. The conditions were the same as those in Figure 4. The most striking conclusion drawn from the experiments is that the flow can be either destabilized, characterized by a large spreading of the jet, or stabilized, by use of a small plate, and the effect is present with the plate located on only one side and in almost any position. Figure 5 gives such a comparison where the distance between the plate and the jet was adjusted while keeping the plate parallel to the jet axis. In this case, the distance the plate must be moved is essentially related to the wave length of the sound wave produced. Although similar stabilizing effects have been observed by others, e.g. Hammitt 1961, with acoustically absorbing baffles at 90°, we believe this is the first case observed where the effect is so pronounced when using a hard reflecting surface. Figure 6 is an example where the plate was positioned 135° to the jet axis. The presence of the plate seems to generate an additional wave system whose origin is located at about the end of the first shock cell.

(b) Total Pressure Measurements

To make measurements in a compressible flow with both a high turbulence level and the presence of shock waves is difficult. This being the case in the near region ($x/D < 15$) of the jet, a pitot tube was used to measure the total pressure and establish some of the basic features of the jet.

A typical variation of the pitot pressure, p_{02}, along the centerline of the jet for a

pressure ratio of 3.8 is shown in Figure 7. The absolute values of p_{02} are divided by the ambient pressure P_a and plotted against the nondimensionalized downstream distance. These results cannot be converted directly into velocity or Mach number because of the unknown entropy increase that has occurred. In steady supersonic flow with a single normal shock wave ahead of the pitot tube, a large pitot pressure correspond to low Mach number, and vice versa. Also shown in the figure is the location of the source for the sound waves observed in the Schlieren photograph (Figure 2b). Two shock cells are clearly identified by the cyclic behavior of the pitot pressure for x/D less than 6. The presence of a complete third cell is not evident here because of the time averaged data taken with the pitot tube. Phase locked Schlieren pictures taken within a single cycle (Krothapalli et al. 1982) show that a complete third shock cell is present only for a small fraction of the time during a cycle. It is observed that the downstream decay of the pitot pressure is considerably accelerated after about 8D, and subsonic flow is found beyond $x/D = 15$.

The conditions at the nozzle exit play a controlling role in the downstream development of the flow, and thus these conditions should be specified in each experiment. In view of this, pitot pressure profiles in the central x,y plane for two different downstream locations close to the nozzle exit ($x/D = 0.1, x/D = 1$) have been made. Figure 8 shows the absolute pitot pressure plotted against the position y. Close to the nozzle exit (i.e. for $x = 0.1D$) the pressure is nearly constant for two-thirds of the nozzle width. A typical profile within the same shock cell at $x/D = 1.0$ is also shown in the figure. If the pitot pressure is converted into Mach number, the profile ($x/D = 1.0$) has a shape quite similar to the one observed within the first few widths of a planar jet. In many practical applications such as thrust augmenting ejectors for short take-off and landing aircraft and certain jet engines, the desired condition at the nozzle exit is a top-hat mean velocity or pitot pressure profile. In this experiment such a profile is obtained.

(c) Mean Velocity Field

While many quantities are of interest in identifying the structure of a turbulent jet, such as the turbulent stress tensor, various velocity correlations, dissipation terms, etc., some measure of the spreading rate of the jet along with mean velocity profiles are very useful for comparison with the behavior of other flows. Most of the mean velocity profiles were obtained using a hot wire in the downstream flow and a hot film in the regions close to

the nozzle exit. Both instruments gave consistent mean velocities (accurate to about 5%) when used to make the same measurement. Measurements were made across the entire jet in some cases in order to establish the symmetry of the flow about its central plane.

Figure 9 shows the measured decay of the mean velocity along the center line of the jet for three different pressure ratios, where U_c is the measured center line velocity and U_0 is the calculated velocity at the center of the nozzle exit (assuming ideally expanded isentropictropic flow). The data presented in the figure are for down-stream stations ranging from $40D$ to $160D$. In all three cases for x/D greater than about 80, the center-line velocity decays as x^{-1} which is depicted by the solid line. This region is usually referred to as the axisymmetric region of a rectangular jet, where the velocity decays at nearly the same rate as that of an axisymmetric jet. Ahead of this region is a two-dimensional type region where the velocity decays at a rate roughly the same as that of a planar jet.

The density of a jet relative to the density of its surroundings has a significant effect on the rate of jet decay (Abramovich 1963). In particular, the greater the ratio of jet density to ambient density, the less rapid will be the jet decay. In the present experiments, the stagnation temperature was equal to the ambient air temperature and therefore the static temperature at the nozzle exit was less than ambient. For example, picking the case $R = 5.4$, the ratio of the exit temperature for an ideally expanded gas to the ambient air temperature was about 0.62, and the ratio of the corresponding densities was therefore 1.61. The effect of increased jet density is evident from a comparison of the data for the lowest and highest pressure ratios. However, for the case of R equal to 3.8 and for x greater than $80D$ a more rapid decay of the velocity is noticed as compared to the lowest pressure ratio. This is principally the result of the strong acoustic excitation present downstream of the nozzle exit (see Figures 2b and 13) which causes an accelerated spreading of the jet.

Figure 10 shows the distribution of mean velocity across the narrow dimension of the jet in the x, y plane at different downstream stations, ranging from $40D$ to $140D$, for the lowest and highest pressure ratios tested. The mean velocity U is normalized at each station with respect to U_c , and the distance Y is normalized by the distance $(x - x_0)$ to the station in question, where x_0 is the distance between the virtual origin of the flow and the nozzle exit. For the case of R equal to 2.7 and for X greater than $40D$, the profiles are geometrically similar within the limits of error for the experiment. Self similarity is also

observed in the profiles for the case of R equal to 5.4, which is represented by the solid line (average of the data points not shown here). In the absence of any strong acoustic interaction with the jet, it appears that the self similar profile broadens with decreasing pressure ratio, i.e the spreading rate increases. From figures 9 and 10 it is observed that a wider profile corresponds to a smaller jet decay. For comparison purposes, the self similar profile of an incompressible rectangular jet of aspect ratio 38 (Gutmark and Wygnanski, 1976) is also shown in the figure and seems to agree well with the case $R = 2.7$. However, the presence of a strong organized wave structure in the near acoustic field of the jet, which occurs at R equal to 3.8 in this experiment, has a considerable effect on the distributions of mean velocity across the jet in the x, y plane. Such profiles are shown in Figure 11 for different down-stream stations ranging from 40 to 140 widths. As before, the distance y is normalized with respect to $(x - x_0)$, where the value of x is different for the two segments $40 < x/D < 80$ and $100 < x/D < 160$. As discussed below, the halfwidth (the width corresponding to the point where the mean velocity is equal to one-half of its value on the axis) in the x, y plane varies linearly with x, with two different slopes, thus producing two different virtual origins (see Figure 15). It is observed that the profiles in each of the two regions are geometrically similar except the scale factor is different for the two. The similarity profile for the downstream flow ($X > 100D$) is quite similar to that observed in Figure 10 for the lowest pressure ratio $R = 2.7$. The unusually rapid spreading of the jet seen in Figure (2b) is the cause of the wider self similar profile in the region $x < 80D$.

Normalized mean velocity profiles in the x, z plane at different downstream locations ranging from $40D$ to $160D$, and for the lowest and highest pressure ratios, are shown in Figure 12. The distance z is again normalized with respect to the distance $(x - x_0)$ where x_0 is the location of the virtual origin (found by extrapolating linearly the variation of the half width in the x, z plane (see Figures 14 and 15). For the case of $R = 2.7$ and for x/D greater than 80, the profiles are again geometrically similar, and have a shape quite similar to that of an axisymmetric jet. A corresponding observation is made for the pressure ratio $R = 5.4$ and is indicated in the figure by the solid line which was drawn through the data points (not shown here). It is observed that the similarity profile for the highest pressure ratio is narrower than that for the lowest. In light of Figures 10 and 12 it appears that the jet spreads at a slower rate with increasing R, except in the range where self acoustic excitation plays a large role. This is consistent with calculations made for the case of

a planar jet by Abramovich 1963. Figure 13 shows the corresponding normalized mean velocity profiles in in the x, z plane for the case of maximum sound radiation, i.e. $R = 3.8$. As before, it appears that the profiles are geometrically similar for large downstream distances. The similarity profile in this case is wider than those shown in Figure 12.

The growth of the jet in x, y and x, z planes is shown in Figures 14 for the lowest and highest pressure ratios, while Figure 15 presents the case for maximum screech sound radiation. The ordinates $y_{1/2}$ and $z_{1/2}$ are the respective distances from the centerline of the jet to the point where the mean velocity in each plane is equal to one-half of its centerline value. The jet in the x, y plane spreads linearly with x and the locus of the half velocity points is given by

$$y_{1/2} = k(x - x_0);$$

where k and x vary with pressure ratio. For the lowest pressure ratio the values of k and x are 0.105 and $-5.3D$ respectively. The corresponding values for the highest pressure ratio are 0.08 and $-21.3D$. In the absence of any dominant discrete sound radiation, a decrease in the spreading rate of about 25% is found for an increase in the pressure ratio from $R = 2.7$ to $R = 5.4$. We may note that for a subsonic rectangular jet, the constant k has a value of about 0.1, and does not change with increasing Mach number (Hsia et al. 1982a). Similar observations were made by Maydew and Reed 1963 in their investigation of turbulent mixing in axisymmetric compressible jets.

It is known that an increase in the Mach number of a supersonic jet results in a decrease in the spreading angle of the mixing region at the boundary of the initial portion of the jet. In most such experiments, the Mach number is increased by increasing the reservoir pressure which causes an increased flow density (if stagnation temperature is kept constant) and the observed effects were attributed to this increased density ratio between the jet and the external gas (Abramovich 1963, Glass 1968). A systematic investigation of the density effects in turbulent mixing layers was carried out by Brown and Roshko 1974. Even though this study deals mainly with two dimensional shear layers, some of the implications of their results apply to the present investigation.

The variation of the half-width in the x, z plane, shown in Figure 14, exhibits a linear increase for downstream distances x greater than about $80D$. However, for x/D

less than 80 it shows a decrease. At some intermediate location the half widths in the two central planes cross each other. The distance from the nozzle exit to the crossing point increases with increasing pressure ratio, except for the special condition of maximum screech sound radiation. Hence, it may be suggested that the two dimensionality of a rectangular supersonic jet is preserved for longer downstream distances with increasing pressure ratio.

Figure 15 shows the variation of the half widths in two central planes with downstream distance for the condition of maximum screech sound radiation ($R = 3.8$). Except for the accelerated growth of $y_{1/2}$ for x/D less than 80, the overall behaviors of the half widths in both planes are quite similar to those observed in Figure 14. In the region $40 < x/D < 80$, the constant k for the $y_{1/2}$ variable assumes a value of about 0.16, while for $x/D > 80$, it has a value of about 0.1. Corresponding values of x_0 were determined in the two regions and used in the normalization of y (i.e. $y/x - x_0$) in plotting the velocity profiles. It is for this reason that the velocity distribution in the x, y plane shows two different self similar profiles, as seen in Figure 11. The reason for the large spreading rate for x/D less than 80, is most probably due to the acoustic excitation present at the end of the third shock cell (i.e. $x/D = 7$). The influence of such excitation on the mean flow seems however to be confined to the region x less than $80D$.

Just as in the previous case, the half width $z_{1/2}$ in the x, z plane grows linearly with x for x greater than about $80D$. However, the location of the virtual origin lies downstream rather than upstream of the nozzle exit. The crossover point (equal half widths in the two central planes) seems to appear much further upstream compared to the cases shown in figure 14. The necking down of the jet in the x, z plane can be seen clearly in the Schlieren photograph shown in Figure 17b. The fact that $y_{1/2}$ and $z_{1/2}$ form parallel or even divergent lines for x greater than $80D$ (see Figures 14 and 15) suggests that true axisymmetry of the mean velocity profiles (profiles are identical in both planes) within the region of interest for these flows is not obtained, which is in contrast to the observation reported by Trenacosta and Sforza 1967, for the case of an incompressible jet where axisymmetry was found for $x > 150D$ for an aspect ratio of 10.

(d) RMS Intensities

As explained in the previous section, many uncertainties appear in attempts to deduce the velocity fluctuation from a hot-wire voltage in a supersonic flow. It is for this reason that the turbulent intensity is defined here as the ratio of the rms of the hot-wire voltage to a mean voltage, $< e > /E$, which allows direct comparison with other work. In incompressible flow this is equal to the ratio $< u > /U$.

Figure 16 shows the downstream variation of the centerline fluctuation intensity $\tilde{e} =< e > /E_0$ for three different pressure ratios. The mean voltage E_0 is obtained from the relation $E_0 = KU_0$, where U_0 is the calculated mean velocity at the center of the nozzle exit plane, assuming ideally expanded isentropic flow, and K is a constant obtained from the calibration plot of the linearized mean hot-wire voltage versus the mean velocity. The value of K is the same for all the data plotted here. Although this approach may not correctly represent the precise downstream variation of $< u > /U$, the relative trends between the various sets of data are expected to be valid. For the underexpanded jet, a hot-film probe was used to make measurements for locations of x less than $40D$, while a hot-wire probe was used for x greater than $40D$. For clarity, a line is drawn through the data points for the case of $R = 3.8$. Also included in the figure are the results for a high speed subsonic ($M = 0.8$) jet, depicted by the solid line which is an average of the data points not shown here. For this case, there is no known acoustic excitation present in the flow, thus giving a basis for comparison with the underexpanded jet data. As seen the magnitude of $\tilde{e}$ increases sharply close to the jet exit, reaches a maximum value at $x/D = 10$, and then decreases monotonically. Such a behavior is common to most of the naturally occurring (non excited) axial turbulence intensity profiles in subsonic jets. Generally, a peak in turbulence intensity occurs near the end of the potential core, which is a result of fluctuations induced by the interaction of the shear layers. The amplitude and position of the peak can be varied significantly by a controlled acoustic excitation of the jet near the nozzle exit plane; see for example Zaman and Hussain 1981. In the self similar region of the underexpanded jet, i.e. for $x/D > 80$, except in the case of $R = 3.8$, the variation of $\tilde{e}$ with x has a behavior similar to that of the subsonic jet. However, the magnitude of $\tilde{e}$ at a given location increases with increasing pressure ratio. For the case of maximum screech sound radiation, i.e. for $R = 3.8$, the profile shows a distinct peak at $x/D = 80$, followed by a faster decay in comparison with the two other cases. It was found that for $15 < x/D < 50$, the magnitude of $\tilde{e}$ decreases like $X^{-1/2}$. As discussed

below, this type of profile seems to be a result of acoustic excitation in the jet. A weak acoustic excitation is also present for the other two pressure ratios (see Figures 2a and 2c), and is exhibited here by a small increase in turbulence intensity at $x/D = 90$, for $R = 2.7$.

For an excited plane jet, it has been shown by Hussain and Thomson 1980, that the excitation appears to directly affect the fluctuation intensity and is more pronounced on the centerline than in the shear layers. From results for acoustically excited axisymmetric and planar jets, it is found that a peak in centerline turbulence intensity occurs in the region of interaction of large scale vortical structures, usually appearing near the end of the potential core (Hussain and Thomson 1980, Zaman and Hussain 1980). As has already been seen in Figure 2b, such structures are present in the region just downstream of the acoustic source. Since a peak is observed in the distribution of $\tilde{e}$ at $X/D = 80$ and in view of the above discussion, one would expect to see large-scale vortical structures in a Schlieren photograph of the flow field at this location. To explore such a possibility, Schlieren photographs for both the x, y and x, z planes, covering the region from the nozzle exit to a downstream location of about $110D$, were taken as shown in Figure 17. Because the available optical setup could not view the entire flow field simultaneously, two photographs in each plane were taken at separate times using a common reference location and assembled as shown in the figure. Together with the cylindrical wave patteren found in the near sound field of the x, y plane (Figure 17a), large scale coherent structures are observed developing along the jet boundary in the region of the acoustic source (also see Figure 2b and 4). Further away from the source no such distinct structures are visible, however, there are large random eddies present on the edges of the jet. Figure 17b shows the flow field of the jet in the x, z plane, and for x/D greater than 50 a distinguishable large scale structure is strongly suggested by the picture. A dotted line presumably representing such a feature is superimposed on the picture. A typical wave length deduced from the picture is found to be equal to about 8cm. On comparing a series of randomly selected pictures of this plane, there does not appear to be a repeatable pattern in their arrangement. However, the "wave length" and overall size of these structures match rather well. A more definitive argument concerning the existence of these structures must include quantitative data. With this objective in mind, oscillograph records of hot-wire outputs and their respective frequency spectra were studied.

Oscillograph records of e fluctuations along the centerline of the jet, for $40 < x/D < 140$, are shown in Figure 18 for $R = 3.8$. All the traces have identical vertical and horizontal scales. As the probe is traversed downstream, low-frequency oscillations dominate the signal, with a recognizable periodicity appearing in the trace at $x/D = 80$. The period can be estimated and is found to be equal to about 1ms (the corresponding frequency is 1000Hz), while the signal at $x/D = 40$, i.e. trace (a), is dominated by more random high frequency fluctuations. Following the arguments of Brown and Roshko 1976, the mean scale of the flow in the x, z plane must increase linearly with $(x - x_0)$. Consequently, it follows that the mean spacing and the mean size of the eddies or large scale structures also increase linearly with $(x - x_0)$. The consequence of increasing spacing leads to a decreasing frequency, which is consistent with the observations made from the oscillograms.

The passage frequency of the large scale structures at a given location can be obtained by studying the frequency spectra of the hot wire signal at that location. Figure 19 shows the frequency spectrum of e for various positions along the centerline of the jet for $15 < x/D < 140$. The horizontal scale is in kilohertz, the range of which varies for some of the plots. For $x/D < 40$ a strong peak around 17.5kHz is observed and found to be equal to the fundamental frequency of the near acoustic field. From a phased locked Schlieren movie of the flow field for a 5mm nozzle (Krothapalli et al. 1982), it was found that the frequency with which the large scale structures pass any station in the x, y plane was identical to the fundamental frequency of the near sound field. Several additional discrete frequencies in the range 0-20kHz are also observed in these plots. With increasing distance downstream, the spectral energy shifts toward the low frequencies. At $x/D = 80$, in addition to other low frequency peaks, a distinct peak at 1048Hz is observed, which is close to the frequency obtained from trace (c) of Figure 18. This frequency then corresponds to the passage frequency of the large scale motions observed in Figure 17b. To further verify this, one can calculate the frequency based on the spacing of two adjacent structures in Figure 17b and the mean convection velocity. The convection velocity of these structures varies from $0.5U_c$ to $0.7U_c$. For $x/D = 80$, we have for the centerline velocity U_c =151m/sec; and assuming an average convection velocity of $0.6U_c$, one obtains a frequency of about 1118Hz, which is quite close to the measured frequency. It is also interesting to note that the ratio of frequencies for the dominant components in the two planes is equal to about 16.7, which

happens to be the aspect ratio of the nozzle.

From the above it may be suggested that acoustic excitation with sources located at $x/D < 10$ serve to generate the large scale structures (or instability waves) above the fine scale random background in both the x, y and x, z planes. When the forcing frequency lies within the instability band, instability waves (or large scale structures) are triggered which undergo a process of growth and then breakdown. It has been shown by Crighton 1973, that a jet with elliptic cross-section and large eccentricity is virtually stable to all temporally growing disturbances; and that in the case of spatially growing disturbances, modes representing sideways oscillation parallel to the major axis have a small growth rate, while those representing a flapping motion parallel to the minor axis have a large growth rate. The disturbances in the above description may be viewed as the vortical structures developing within the shear layers of the jet. The growth and break down or decay of these disturbances is generally reflected in the amplitude distribution of the rms intensity along the centerline of the jet. In light of this discussion it is perhaps logical to suggest that the amplitude of the disturbances in the x, y plane increases monotonically, reaches a maximum at some distance x less than $15D$, and then rapidly decays, while the disturbances in the x, z plane achieve their maximum amplitude at $x/D = 80$ and then decay as shown in Figure 16.

With regard to the forcing frequency (self excited in this case), one can calculate the Strouhal number ($St = fD/U_0$) and compare it with the value for any similar flow situation to see whether it falls within an instability band. Although the flow near the nozzle exit is complicated by the presence of a shock cell structure, we are concerned here mainly with the flow in the shear layers surrounding the shock cells. This part of the flow is mainly compressible and subsonic. Lacking data on the instability characteristics of such a flow, it is to a certain extent reasonable to compare the present data with the instability characteristics of a plane incompressible air jet. Sato 1960, experimentally investigated the instability of a plane air jet, emerging from a laminar channel flow, in the presence of an imposed transverse acoustic perturbation from a loud speaker placed perpendicular to the flow direction. The most unstable jet Strouhal number $St = fD/U_0$ (D=width of the nozzle) for antisymmetric modes was observed to be equal to 0.14. For the disturbances in the x, y plane with the observed frequency of 17,500Hz and using the

same definition (fD/U_0), the Strouhal number is found to be 0.12, which is within 15% of the most unstable Strouhal number of an incompressible plane jet. Similarly, the Strouhal number for the disturbances in the plane containing the long dimension of the nozzle, i.e. x, z plane, was also calculated, using the observed frequency of 1048Hz and the long dimension of the nozzle L =50mm, and found to be again equal to 0.12. Thus, suggesting that the most unstable Strouhal numbers in the two planes are the same, except the growth rates of the disturbances, as suggested by Crighton 1973, are different in different planes. It is also interesting to note that the maximum screech sound radiation occurs when the Strouhal number equals to the most unstable Strouhal number of the plane incompressible jet. To further verify this, Strouhal numbers for the maximum screech sound radiation were calculated using available data in the literature and the results are tabulated, together with the present data, in Table 1. Data are also included in the table for axisymmetric jets. It appears that the most unstable Strouhal number for rectangular jets (based on the criteria of maximum screech sound radiation) appears to be in the range 0.11- 0.14, which surprisingly falls within the range of a plane incompressible jet. For axisymmetric jets, the Strouhal number ($St = fD/U$, D is the diameter of the nozzle) appears to be in a range 0.24 - 0.28, which is close to the value 0.3, the so-called "preferred mode" of a jet (Zaman & Hussain 1980, Crow & Champagne 1971).

Profiles of $\tilde{e}$ in the x, y plane at different downstream locations for $R = 3.8$, are shown in Figure 20. In general the profiles shapes are similar to the ones found for two dimensional jets, where geometrical similarity exists in the outer flow and a distinct saddle shape appears at small values of x/D. For values of x/D greater than 80, the profiles tend toward axisymmetry, and seem to approach complete self similarity with increasing downstream distance. The profiles for $x/D < 80$ are much broader in the η variable in comparison with the profiles for $x/D > 80$. It appears that, when comparing the $\tilde{e}$ profiles in Figure 20 with the corresponding mean velocity profiles in Figure 11, the major influence of the acoustic excitation is present up to a downstream distance of about $80D$. Profiles of $\tilde{e}$ in the x, z plane are shown in Figure 21. For x/D greater 80, it appears that the $\tilde{e}$ profiles assume geometric similarity. This observation in conjunction with the self similar mean velocity profiles for $x/D > 80$ suggest that the flow in the x, z plane reaches a self similar state. In light of these measurements (both mean and rms profiles) it may be suggested that the flow field of a rectangular jet reaches self similar states in both planes at locations

downstream of the crossover point. However, the shapes of the self similar profiles are different in the two planes. Furthermore, it appears that complete axisymmetry of the jet may not be reached within a reasonable (of engineering interest) distance downstream. The profiles of $\tilde{e}$ at different downstream locations for $R = 2.7$ and 5.4 in both the x, y and x, z planes (not shown here), show a similar behavior as discussed above, except for the enhanced effects of acoustic excitation.

CONCLUSIONS

An objective of this work was to study the mean and turbulent velocity fields of an underexpanded rectangular jet of moderate aspect ratio. While investigating this problem, we encountered two major factors influencing the overall flow field of the jet. One is to be expected and is the effect of the density ratio between the jet and the ambient air. The second factor, typical of underexpanded jets, is the generation of "screech" tones and their influence on the structure of the jet. Although discrete tones or "screech" tones are found in the near sound field of the jet for all pressure ratios above the critical pressure ratio (i.e. $R = 1.9$), they are most intense and have greatest effect on the overall flow field only in the range of pressure ratios from 3 to 4. The maximum screech sound radiation occurs in this experiment at a pressure ratio of 3.8. When the jet is operating outside this range of pressure ratios, the influence of screech tones is less important, as compared to the effects of varying density, on the mean and turbulence velocity fields of the jet.

From the Schlieren photographs studied, the following observations are made. For the condition of maximum screech sound radiation, a very strong organized cylindrical wave pattern is observed, which originates alternately from each side of the jet. The source for this wave system is located approximately at the end of the third shock cell and serves as an acoustic excitation for the entire jet flow field. Associated with the presence of the wave system is an increased spreading rate of the jet in the plane containing the small dimension of the nozzle. When the frequency of the acoustic excitation lies within the instability band for a plane incompressible jet, it serves to introduce large scale coherent structures in the turbulent flow. Such structures are observed here in both planes of the jet. However, in the x,y plane they appear just downstream of the acoustic source, i.e. at $x/D = 10$, while in the x, z plane they are observed at downstream locations of x/D greater than about 60. The existence of these large scale structures at different downstream locations in the two planes was also confirmed by oscillograph records of hot-wire signals and their respective frequency spectra. The Strouhal number for these organized motions was found to be equal to 0.12, which is close to the most unstable frequency for the antisymmetric modes of the planar incompressible jet. The frequencies in the two planes thus scale with the aspect ratio of the nozzle. These observations are supported by the theoretical work

of Crighton 1973, who studied the stability of a jet with an elliptic cross-section. He found that in the case of spatially growing disturbances, modes representing sideways oscillation parallel to the major axis, or long dimension of the nozzle, have a small growth rate, while those representing a flapping motion parallel to the minor axis, or small dimension of the nozzle, have a large growth rate.

The mean and rms intensity profiles, for x/D greater than 80, in both the central x, y and x, z planes, exhibit separate geometrical similarity in their respective planes, thus suggesting that complete axisymmetry (i.e. identical profiles in both planes) of the jet may not be achieved within a reasonable distance downstream. This is in contrast to ones intuitive notion that a rectangular jet should reache a complete axisymmetric state in a relatively short distance downstream of the nozzle exit.

In the absence of acoustic excitation with increasing pressure ratio (increase in reservoir pressure), a decrease in the spreading angle of the jet was observed. Similar observations have also been made in studies of other supersonic shear layers and is associated with the increasing density of the jet.

REFERENCES

Abramovich, G.N. 1963. The theory of turbulent jets. M.I.T. Press, Cambridge, Mass.

Brown, G.L., and Roshko, A. 1974. On density effects and large structure in turbulent mixing layers. 64, 745-816.

Crighton, D.G. 1973. Instability of an elliptic jet. J. Fluid Mechanics. 59, 655-672.

Crow, S.C., and Champagne, F.H. 1971. Orderly structure in jet turbulence. J. Fluid Mechanics. 48, 567-

Davies, M.G., and Oldfield, D.E.S. 1962. Tones from a chocked axisymmetric jet. ACOUSTICA. 12, 257-277.

Glass, R.D. 1968. Effects of acoustic feedback on the spread and decay of supersonic jets. AIAA Journal. 6, 1890-1897.

Gutmark, E., and Wygnanski, I. 1976. The planar turbulent jet. J. Fluid Mechanics. 73, 465-495.

Hammitt, G.H. 1961. The oscillation and noise of an overpressure sonic jet. J. Aerospace Sciences. Vol. 28, No. 9, 673-680.

Harper-Bourne, M., and Fisher, J.M. 1973. The noise from shock waves in supersonic jets. AGARD CP-131.

Hsia, Y., Krothapalli, A., Baganoff, D., and Karamcheti, K. 1982a. Effects of Mach number on the development of a subsonic rectangular jet. AIAA Paper No. 82-0219.

Hsia, Y., Krothapalli, A., Baganoff, D., and Karamcheti, K. 1982b. The structure of a subsonic compressible rectangular jet. Joint Institute for Aeronautics and Acoustics Report TR-43, Stanford University.

Hussain, F.M.K.A., and Thompson, A.C. 1980. Controlled symmetric perturbation of the plane jet: An experimental study in the initial region. J. Fluid Mechanics, 100, 397-431.

Krothapalli, A., Baganoff, D., and Karamcheti, K. 1981. On the mixing of a rectangular jet. J. Fluid Mechanics., 107, 201-220.

Krothapalli, A., Baganoff, D., Hsia, Y., and Karamcheti, K. 1981. Some features of tones generated by an underexpanded rectangular jet. AIAA Paper No. 81-0060.

Krothapalli, A., Baganoff, D., Hsia, Y., and Karamcheti. 1982. On the mechanisms of tone generation in an underexpanded rectangular jet. In preparation.

Lassiter, W.L., and Hubbard, H.H. 1956. The near noise field of static jets and some model studies of devices for noise reduction. NACA Report 1261.

Lowson, V.M., and Ollerhead, B.J. 1968. Visualization of noise from cold supersonic jets. The J. of the Acoustical Society of America, 44, 624-630.

Maydew, C.R., and Reed, F.J. 1963. Turbulent mixing of compressible free jets. AIAA Journal, 1, 1643-1644

Poldervaart, J.L.,Wijnands, J.P.A., and Bronkhurst, L., 1973. Aerosonic games with the aid of control elements and externally generated pulses. AGARD CP-131.

Powell, A., 1953a. On the noise emanating from a two dimensional jet above critical pressure. The Aeronautical Quarterly, IV, 103-122.

Powell, A., 1953b. On the mechanism of chocked jet noise. Proc. Phy. Soc. London, Series B, 66, 1039-1056.

Powell, A., 1953c. The noise of chocked jets. J. of Acoustical Society of America, 25, 385-389.

Morkovin, M.V., 1981. Private Communication.

Sato, H., 1960. The stability and transition of a two dimensional jet. J. of Fluid Mechanics, 7, 53-80.

Schlichting, H. 1980. Boundary layer theory. McGraw Hill.

Sherman, M.P., Glass, R.D., and Dulleep, G.K. 1976. Jet flow field during screech. Applied Scientific Research, 32, 283-303.

Thomson, A.P. 1974. Compressible fluid dynamics. McGraw Hill, Chapter 4, pp 222.

Westley, R., and Woolley, H.J. 1973. The near field sound pressure of a chocked jet during screech cycle. AGARD CP-131.

Zaman, Q.M.B.K., and Hussain, F.M.K.A. 1980. Vortex pairing in a circular jet under controlled excitation. Part 1. General jet response. J. Fluid Mechanics, 101, 449-491.

Zaman, Q.M.B.K., and Hussain, F.M.K.A. 1981. Turbulence suppression in free shear flows by controlled excitation. J. Fluid Mechanics, 103, 133-159.

Table 1

Geometry of the nozzle	Characteristic dimension D	Pressure ratio velocity U	Frequency Hz	St= fd/U	comments
Rectangular AR=16.7	0.3cm	3.8 430 m/s	17,500	0.12	Present results
Rectangular AR=10	0.5cm	3.5 418m/s	10,000	0.12	Present results
Rectangular AR=12.75	0.635cm	3.67 423m/s	7,375	0.11	Hammitt
Rectangular AR=5.83	0.305cm	3.67 423m/s	18,750	0.135	Powell
Rectangular AR=1.7	0.18cm	3.17 403m/s	31,640	0.14	Powell
Axisymmetric	2.54cm	3.67 423m/s	4,000	0.24	Powell
Axisymmetric	1.27cm	4.0 435m/s	9,428	0.275	Sherman et al.

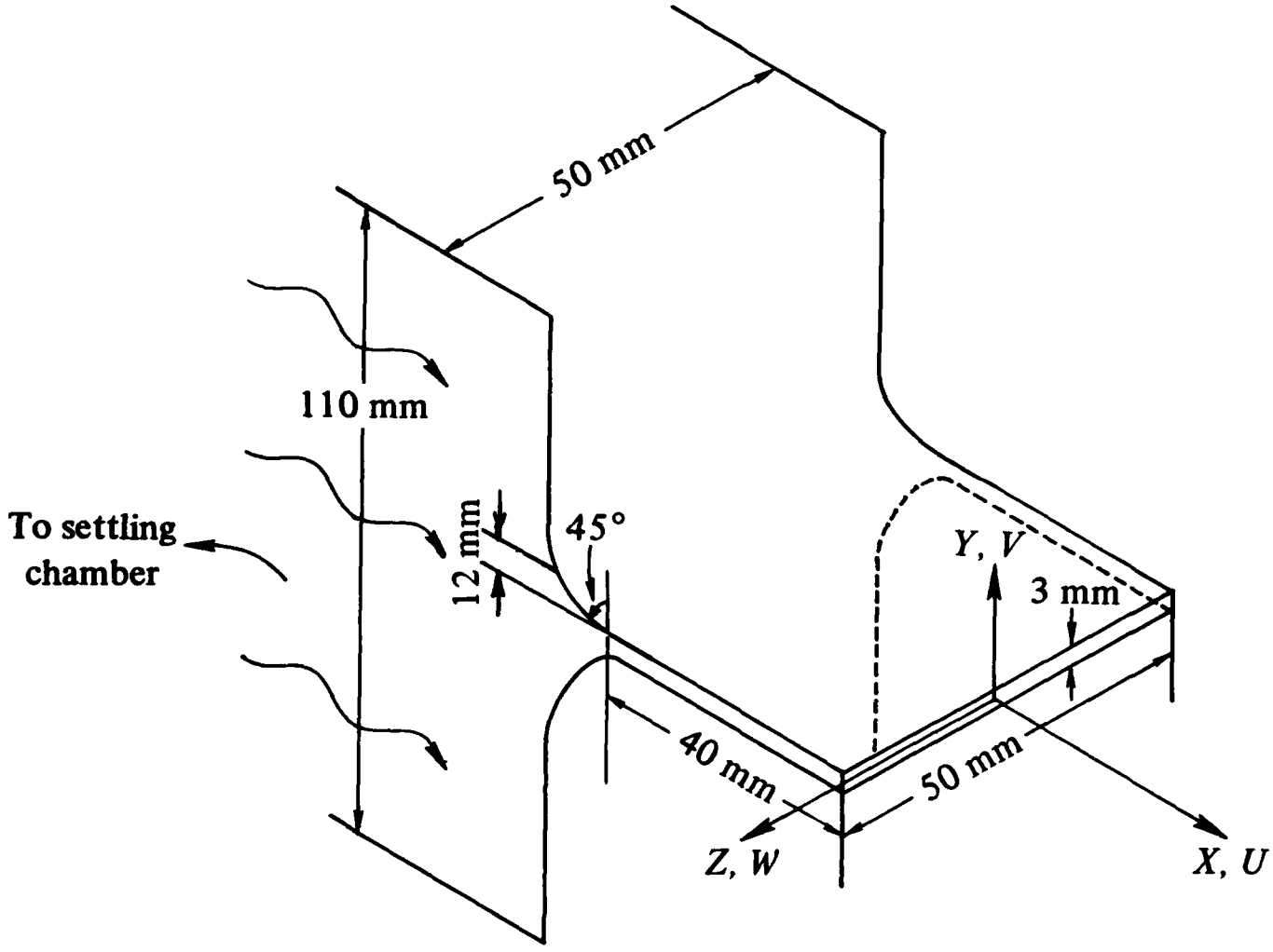

Figure 1. Schematic diagram of rectangular nozzle and entry region.

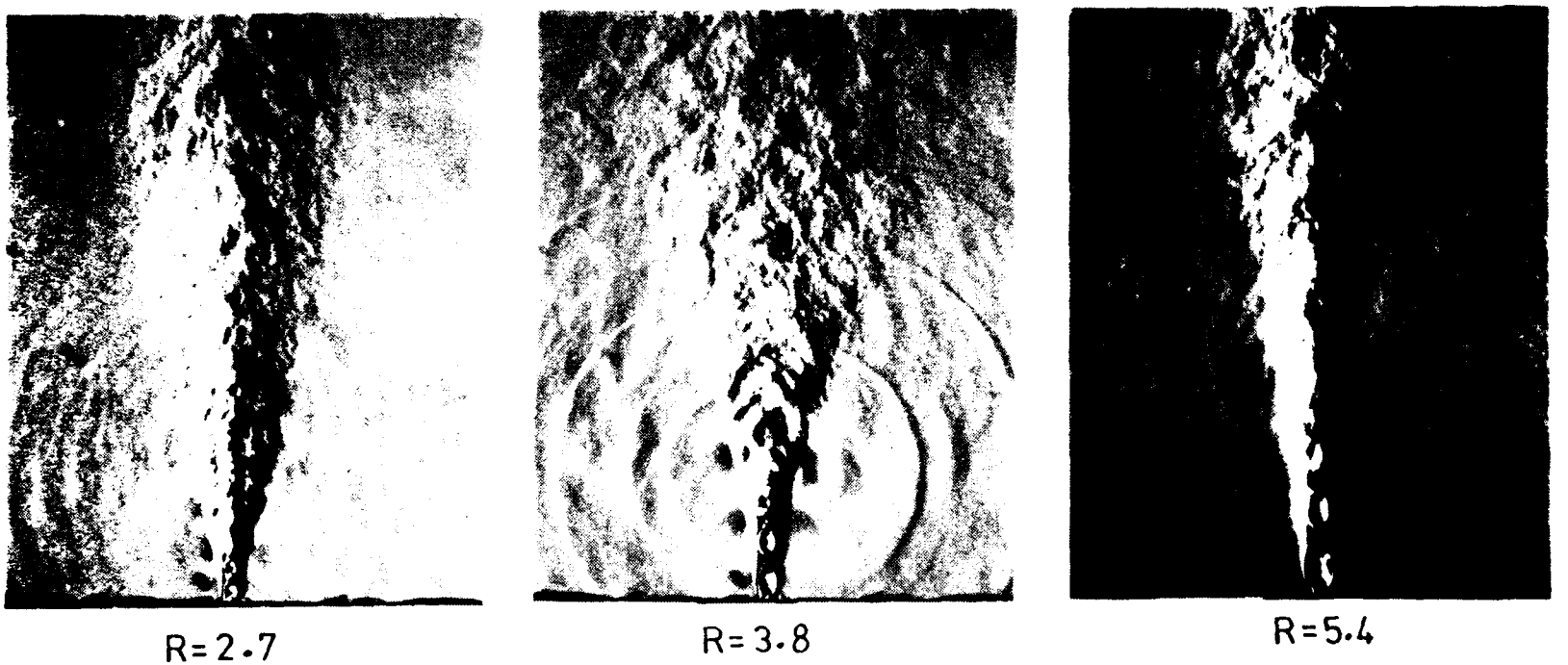

Figure 2. Schlieren pictures of the jet in the x, y plane. $AR = 16.7, D = 3\text{mm}$.

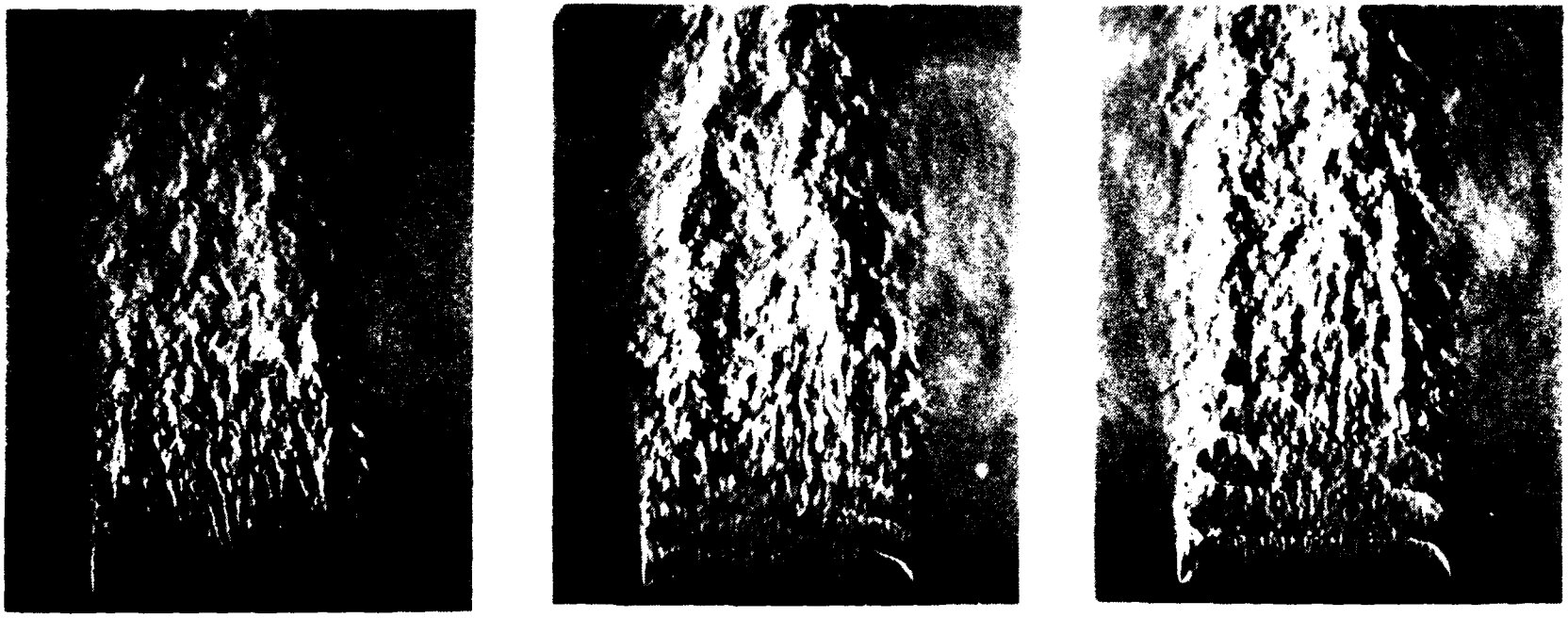

Figure 3. **Schlieren pictures of the jet in the x, z plane.** $AR = 16.7, D = 3\text{mm}$.

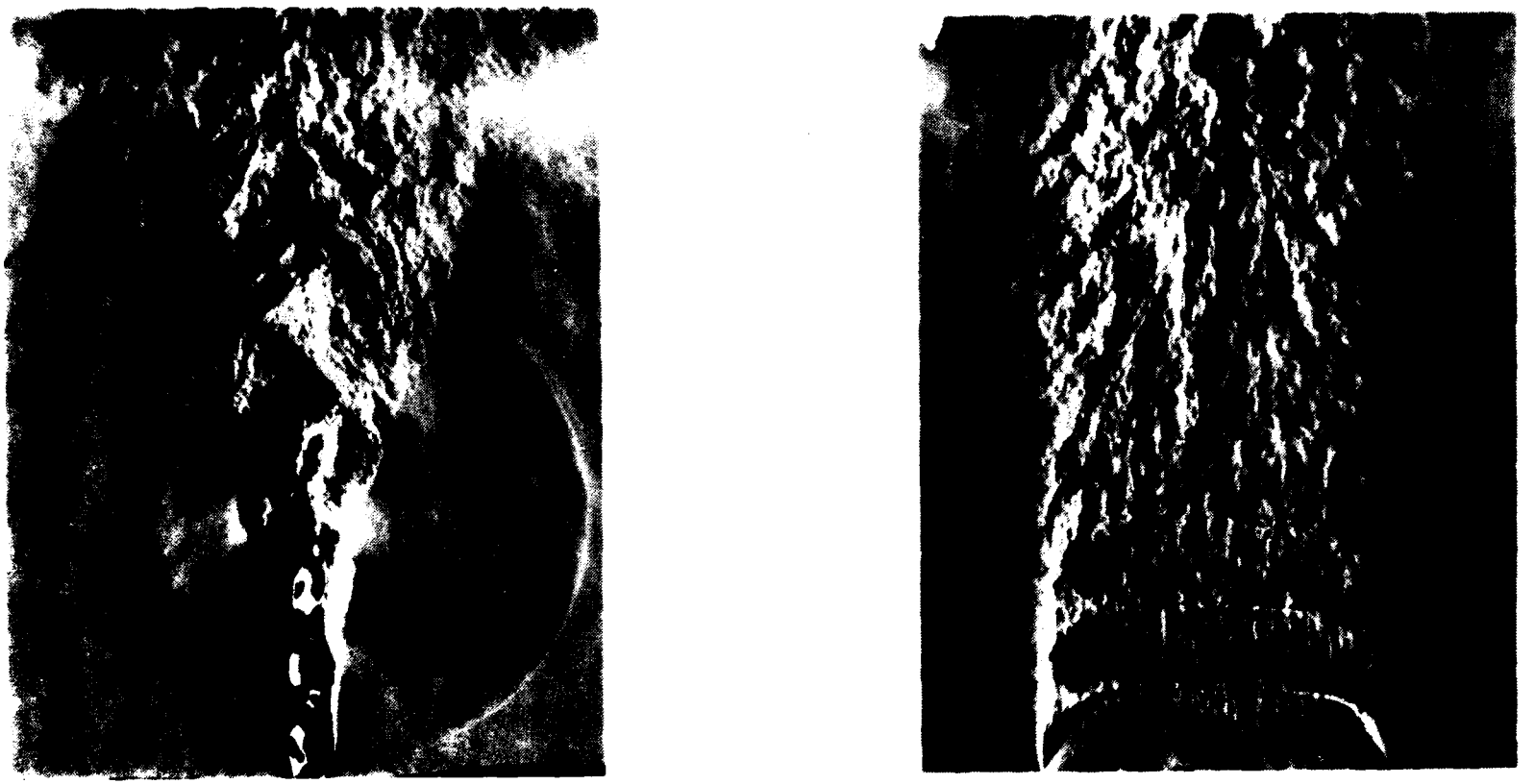

Figure 4. **Schlieren pictures of the jet in both x, y and x, z planes.** $AR = 10, D = 5\text{mm}$.

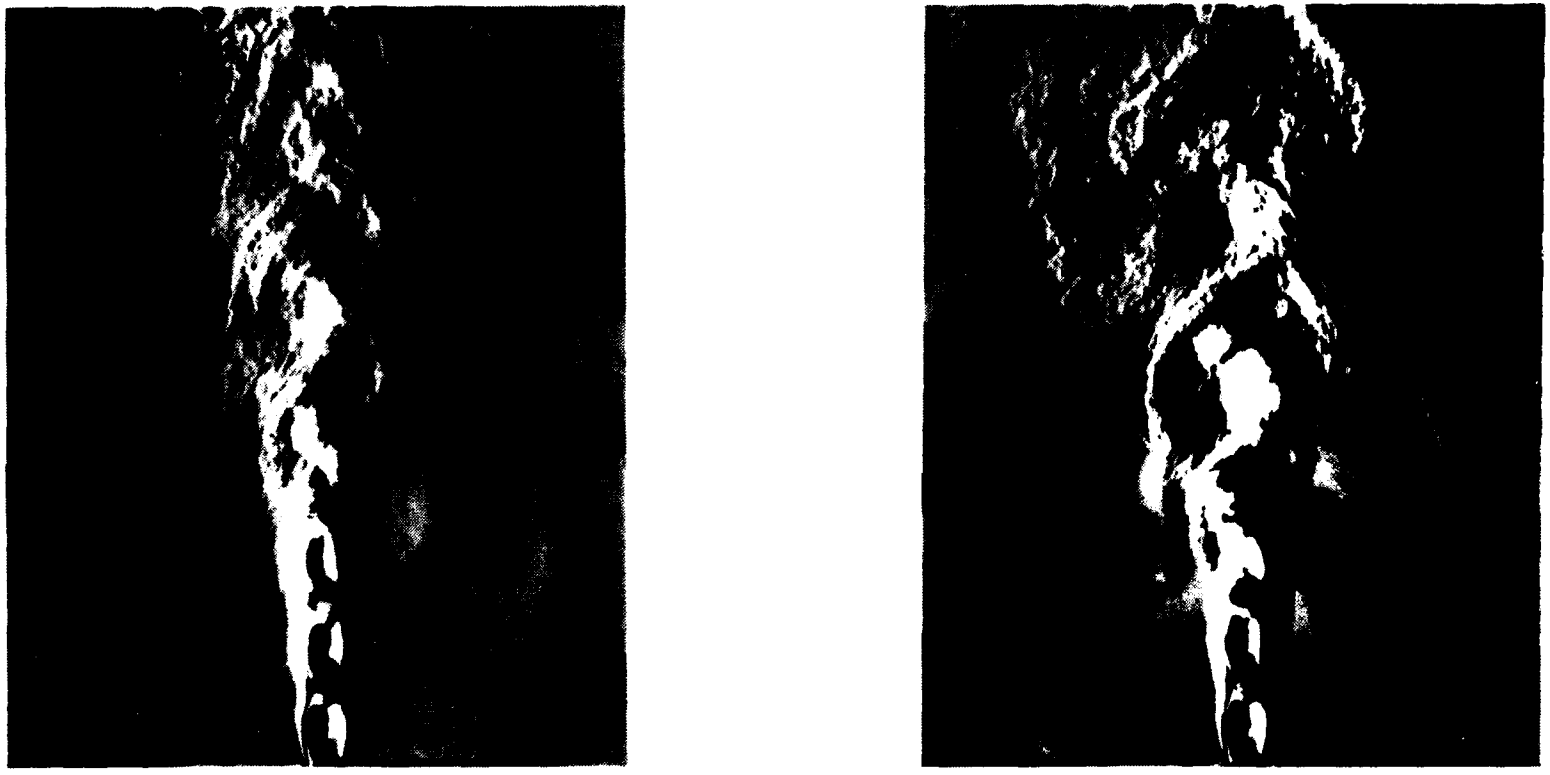

Figure 5. **Schlieren pictures of the jet in the x, y plane, with a reflecting surface placed parallel to the jet axis. $AR = 10, D = 5$mm.**

Figure 6. **Schlieren picture of the jet in the x, y plane with a reflecting surface placed at 135 to the jet axis.** $AR = 10, D = 5$mm.

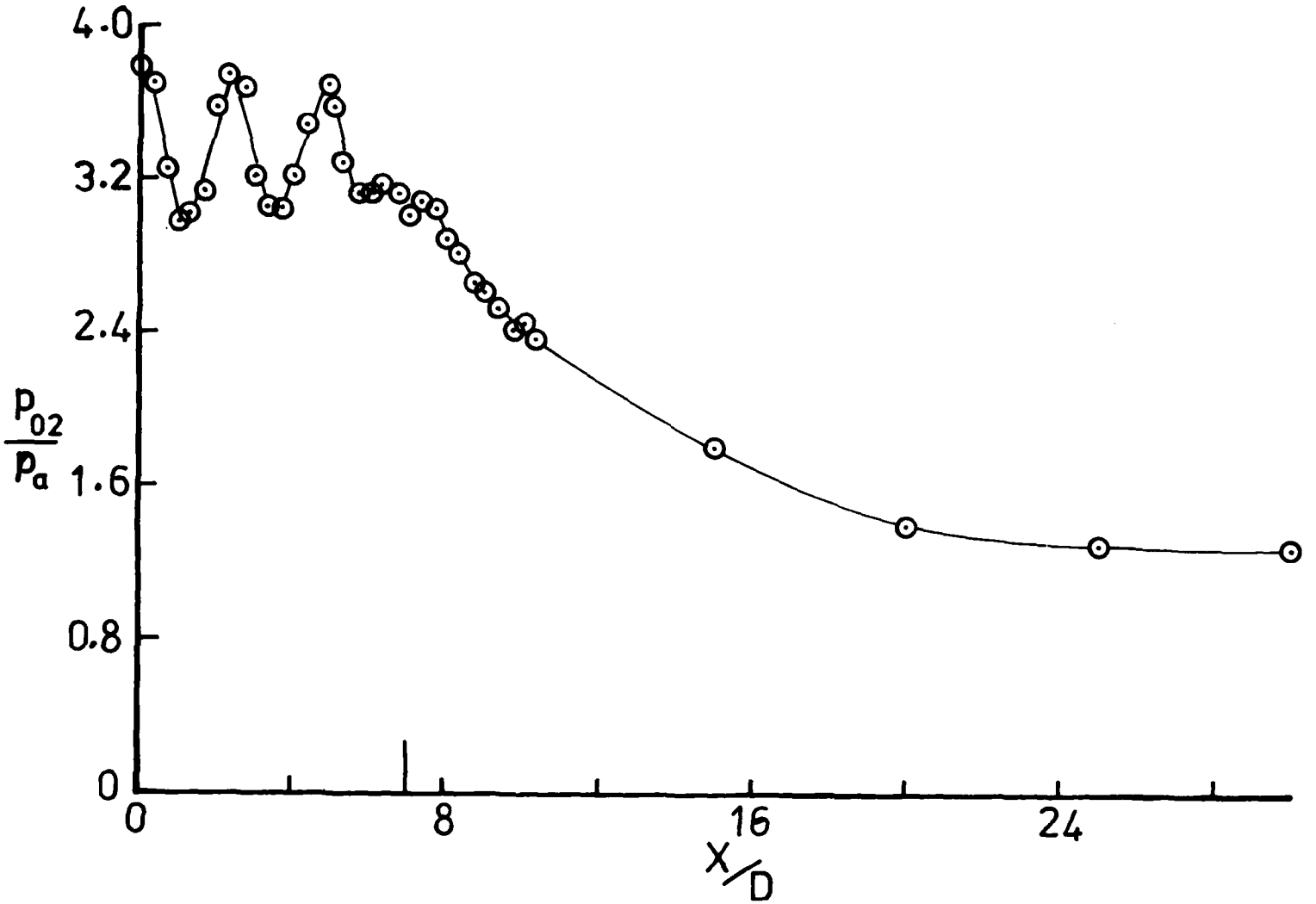

Figure 7. **Variation of the pitot pressure along the center line of the jet.** $R = 3.8$.

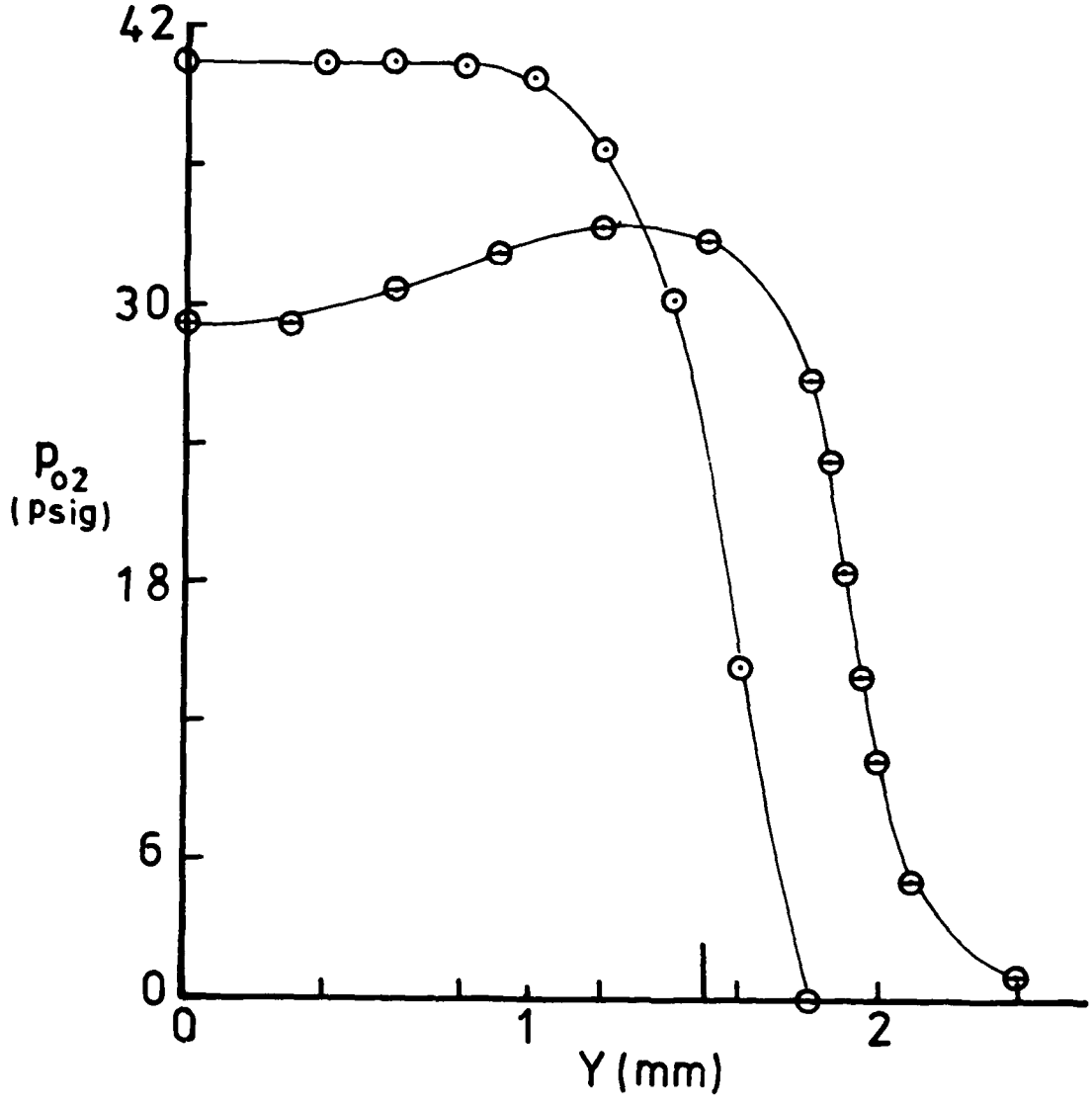

Figure 8. **Pitot pressure profiles in the x,y plane near the nozzle exit, $Z = 0$.** $\odot, x/D = 0.1; \ominus, x/D = 1.0$.

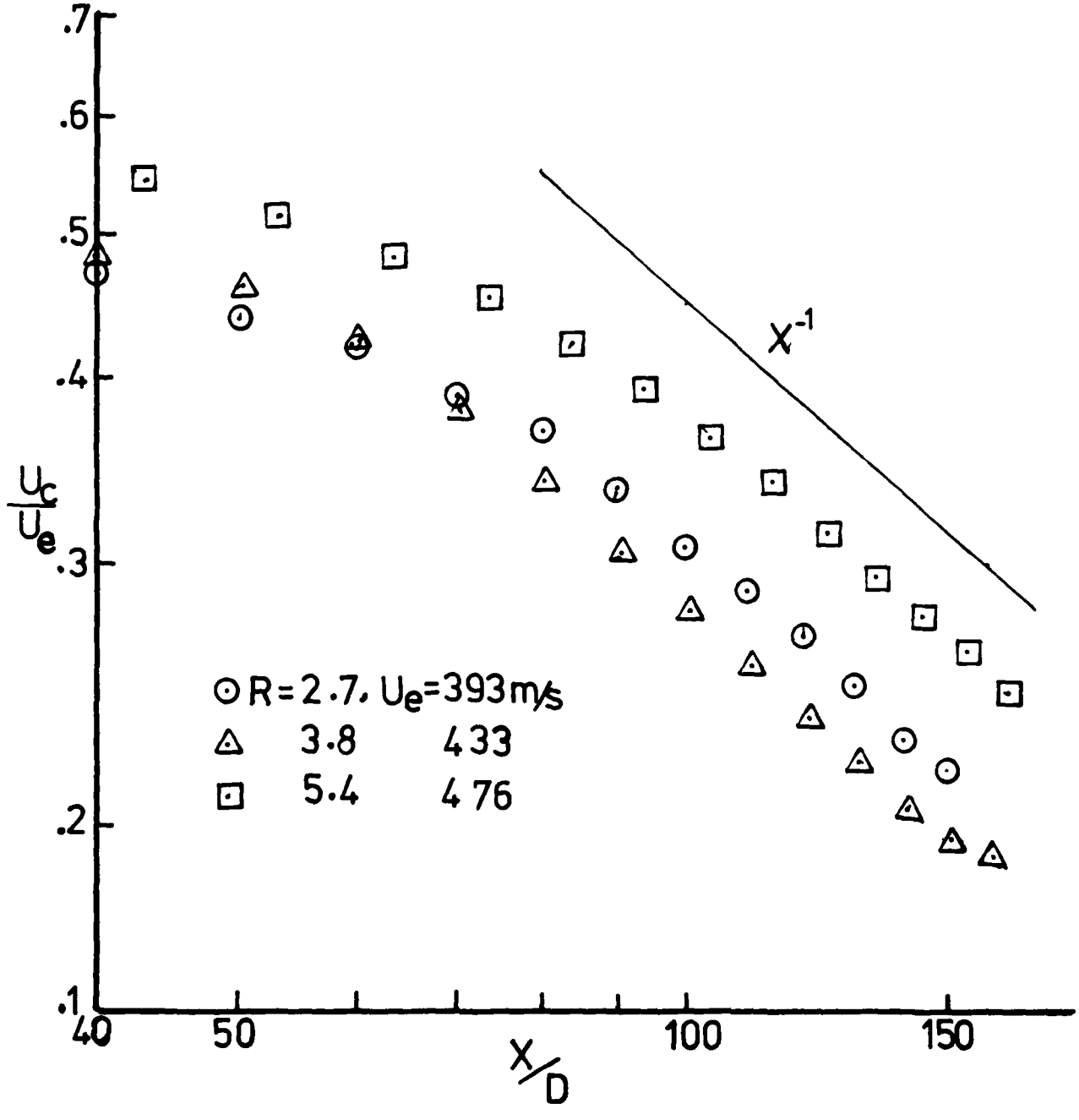

Figure 9. **The decay of the mean velocity along the centerline of the jet.** ⊙, $R = 2.7$; △, $R = 3.8$; ⊡, $R = 5.4$.

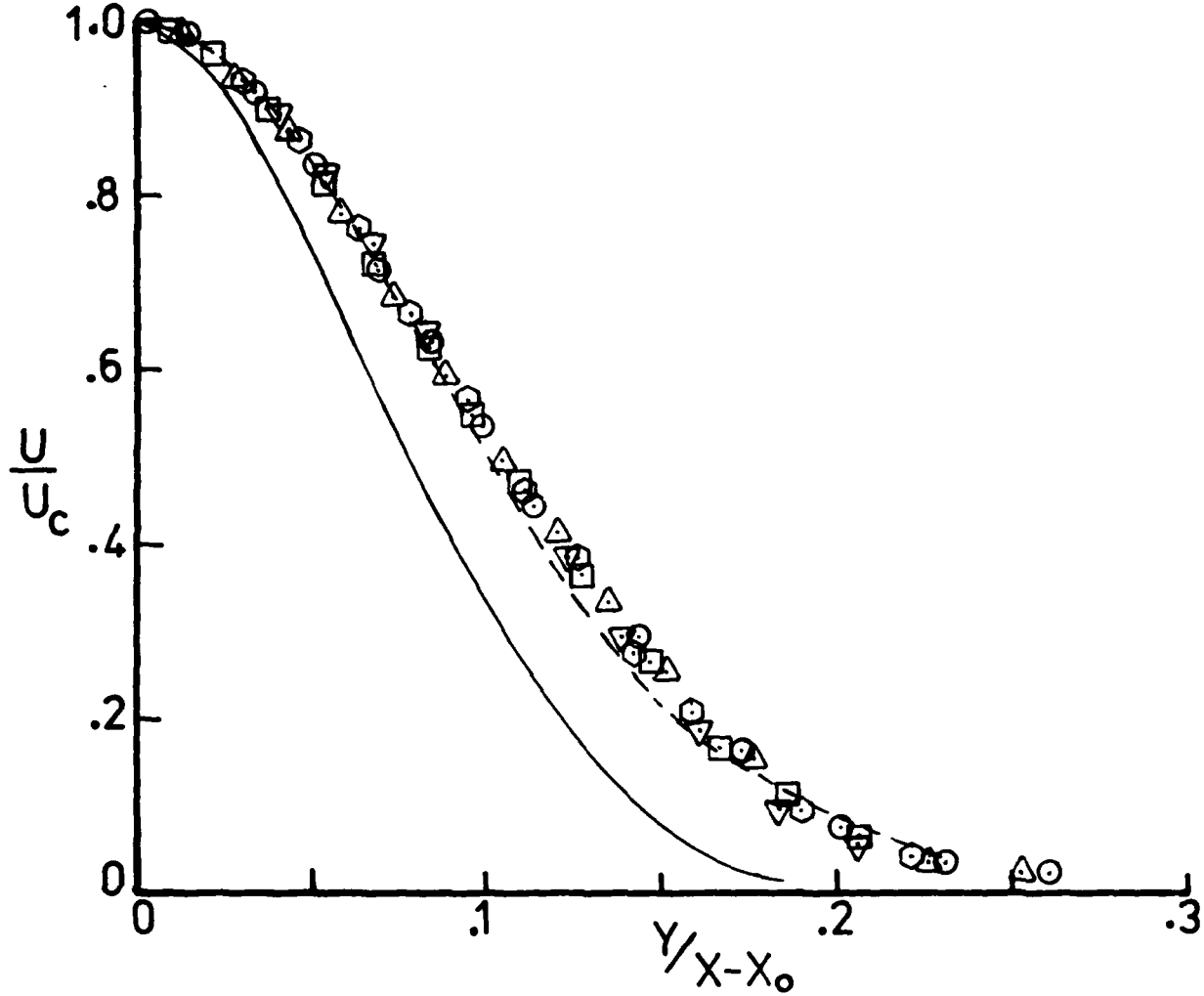

Figure 10. **Mean velocity profiles in the x, y plane, $z = 0$.** $R = 2.7$; ⊙, $x/D = 40$; △, $x/D = 60$; ⊡, $x/D = 80$; ⬡, $x/D = 100$; ▽, $x/D = 140$; ———, $R = 5.4$; – – – –, $AR = 38$, Gutmark and Wygnanski (1976).

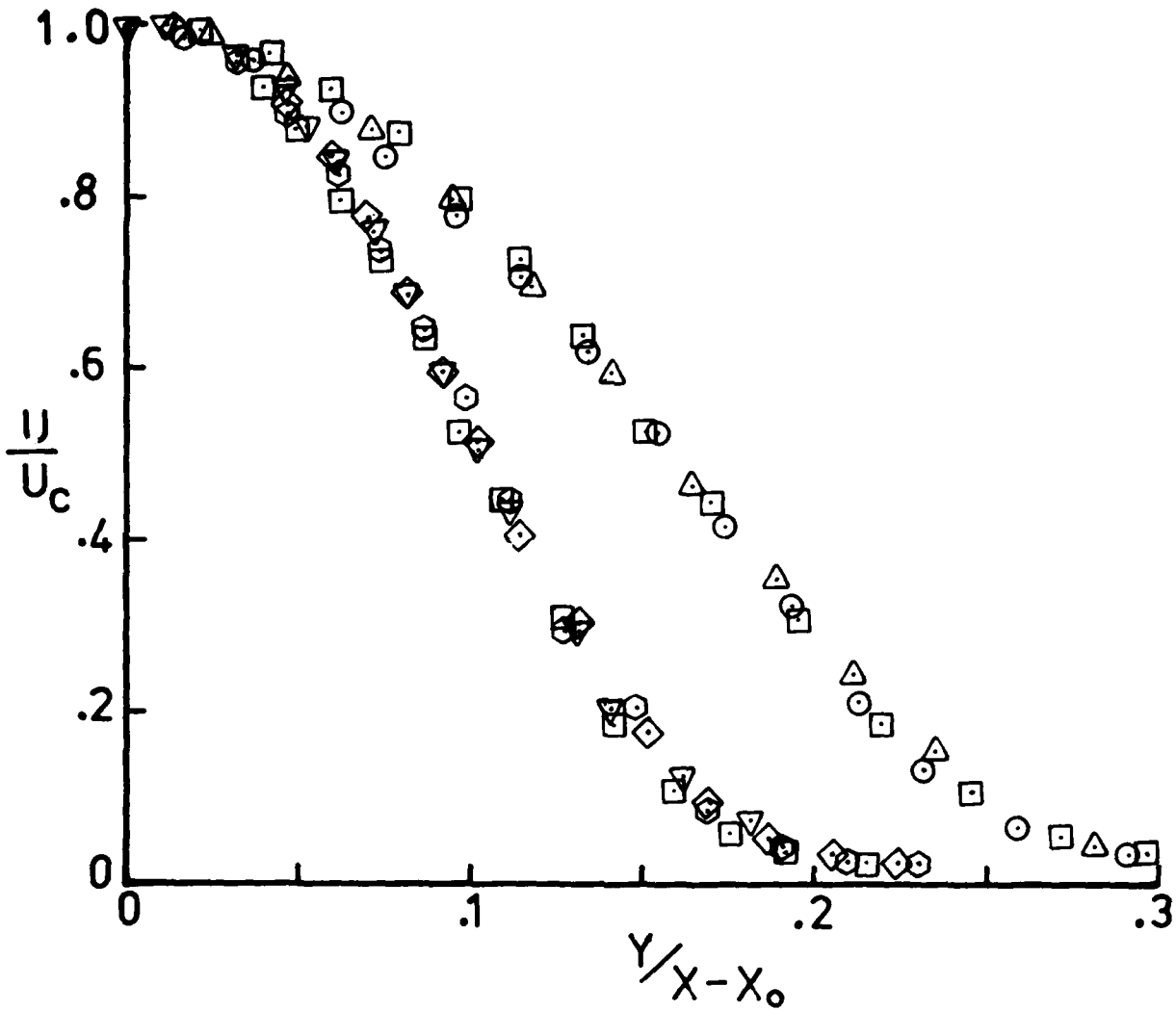

Figure 11. **Mean velocity profiles in the x, y plane, $z = 0$.** $R = 3.8$; ▽, $x/D = 40$; △, $x/D = 60$; □, $x/D = 80$; ⬡, $x/D = 100$; ◇, $x/D = 120$; ▽, $x/D = 140$.

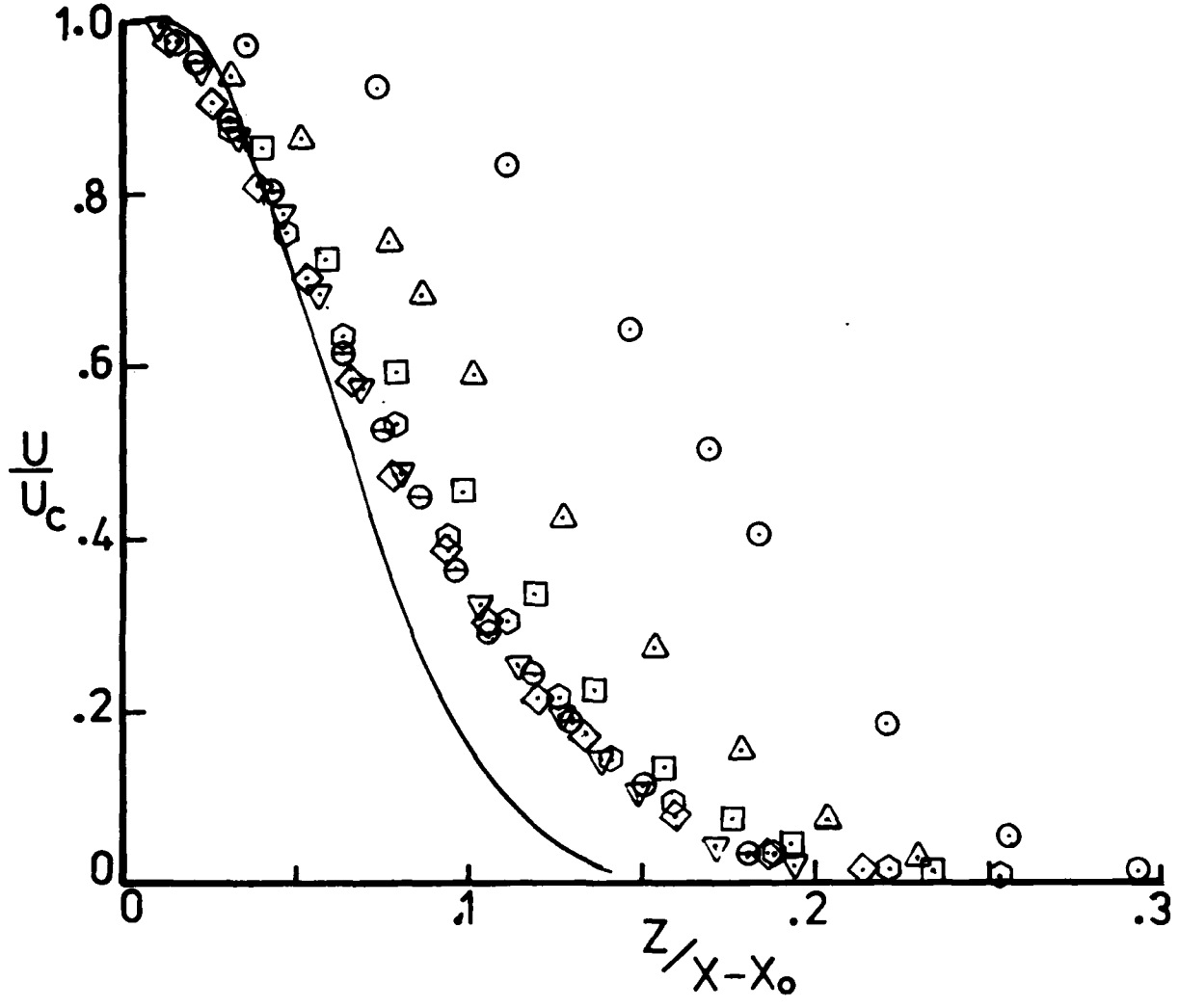

Figure 12. **Mean velocity profiles in the x, z plane, $y = 0$.** $R = 2.7$; ⊙, $x/D = 40$; △, $x/D = 60$; ⊡, $x/D = 80$; ⬡, $x/D = 100$; ◇, $x/D = 120$; ▽, $x/D = 140$; ○, $x/D = 150$; ———, $R = 5.4$.

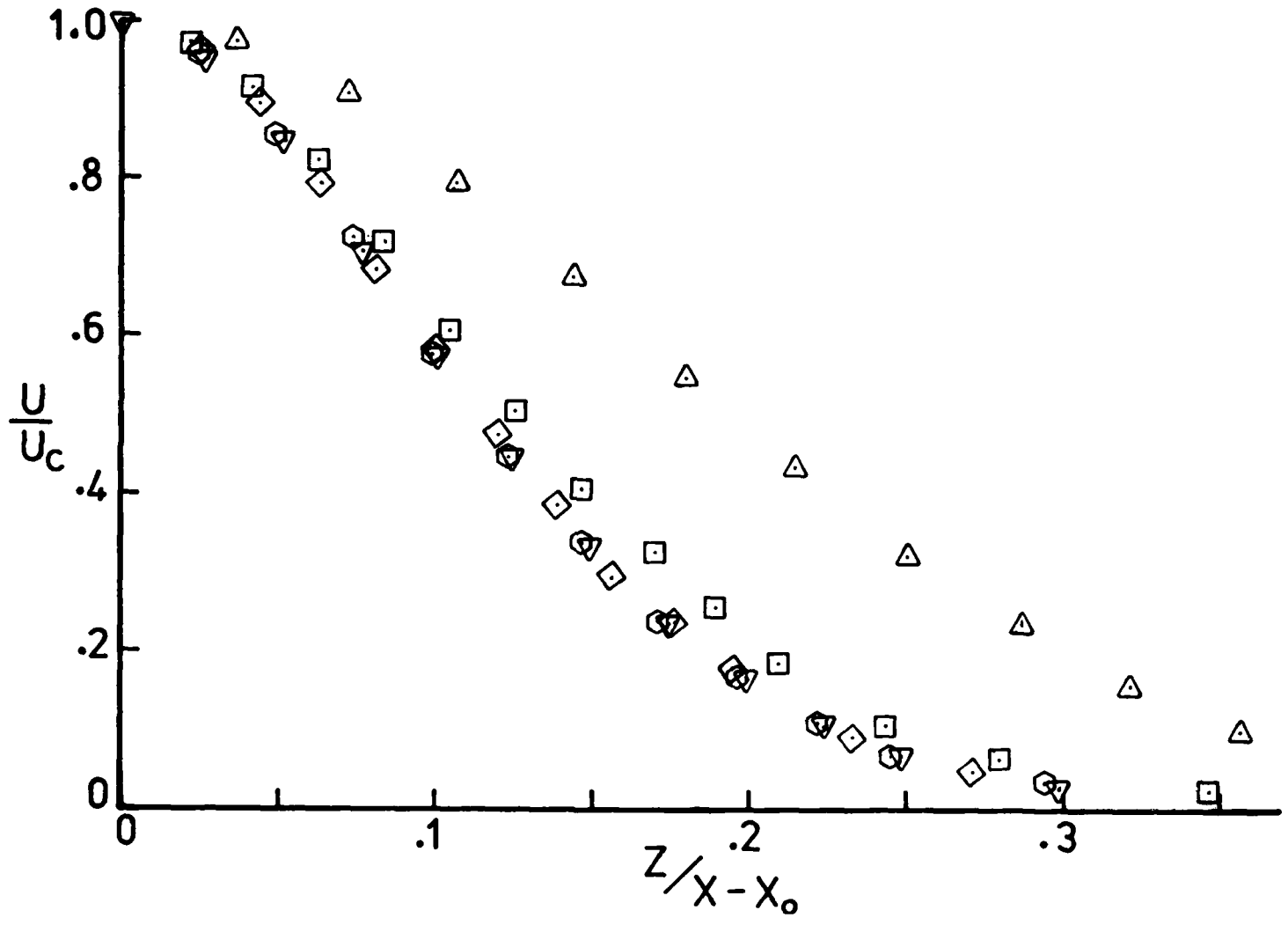

Figure 13. **Mean velocity profiles in the x, z plane, $y = 0$.** $R = 3.8$; △, $x/D = 60$; ⊡, $x/D = 80$; ⬡, $x/D = 100$; ◇, $x/D = 120$; ▽, $x/D = 140$.

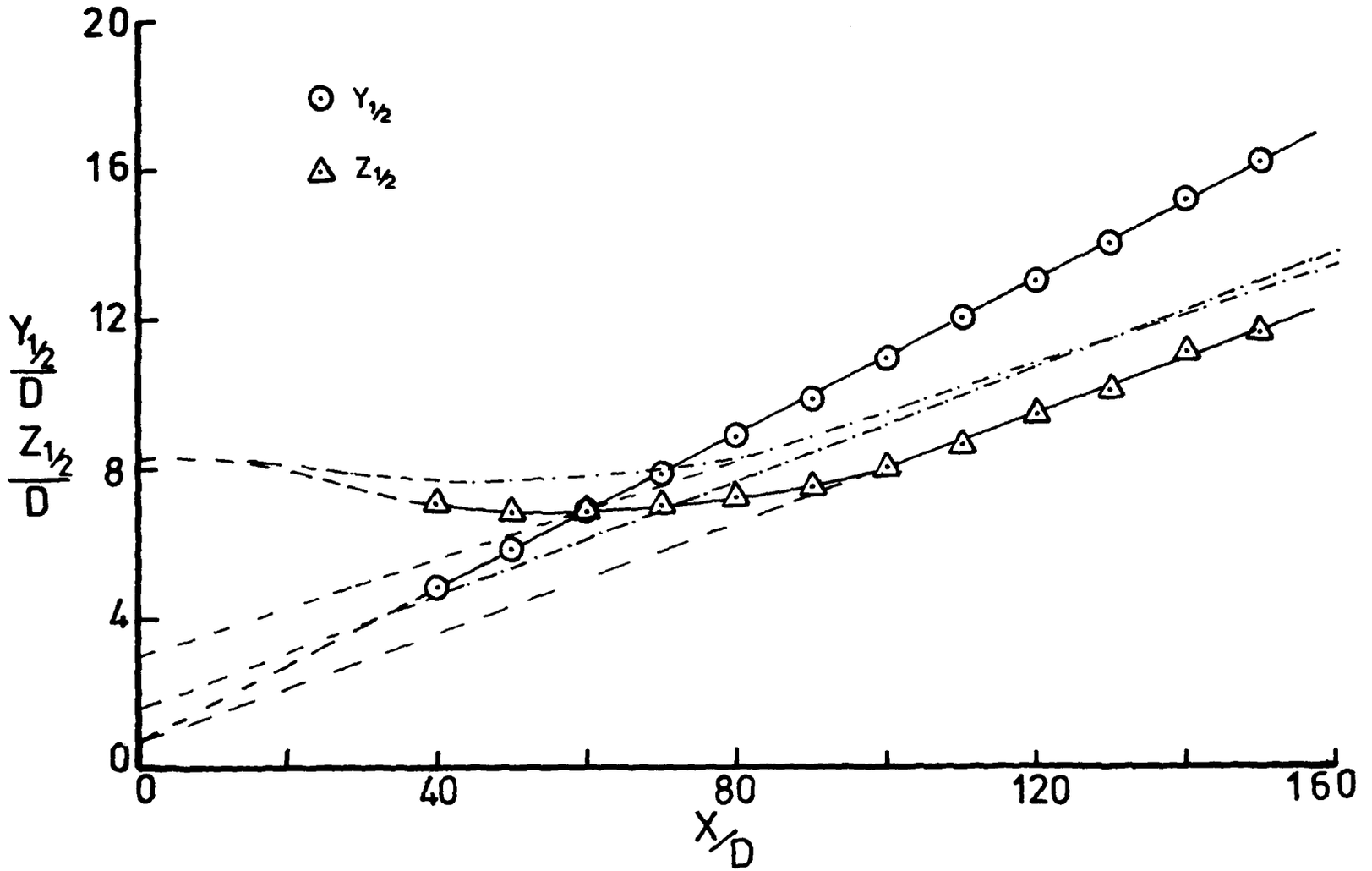

Figure 14. **Growth of a rectangular jet with down stream distance.** ⊙ , △ , $R = 2.7$, ----, $R = 5.4$.

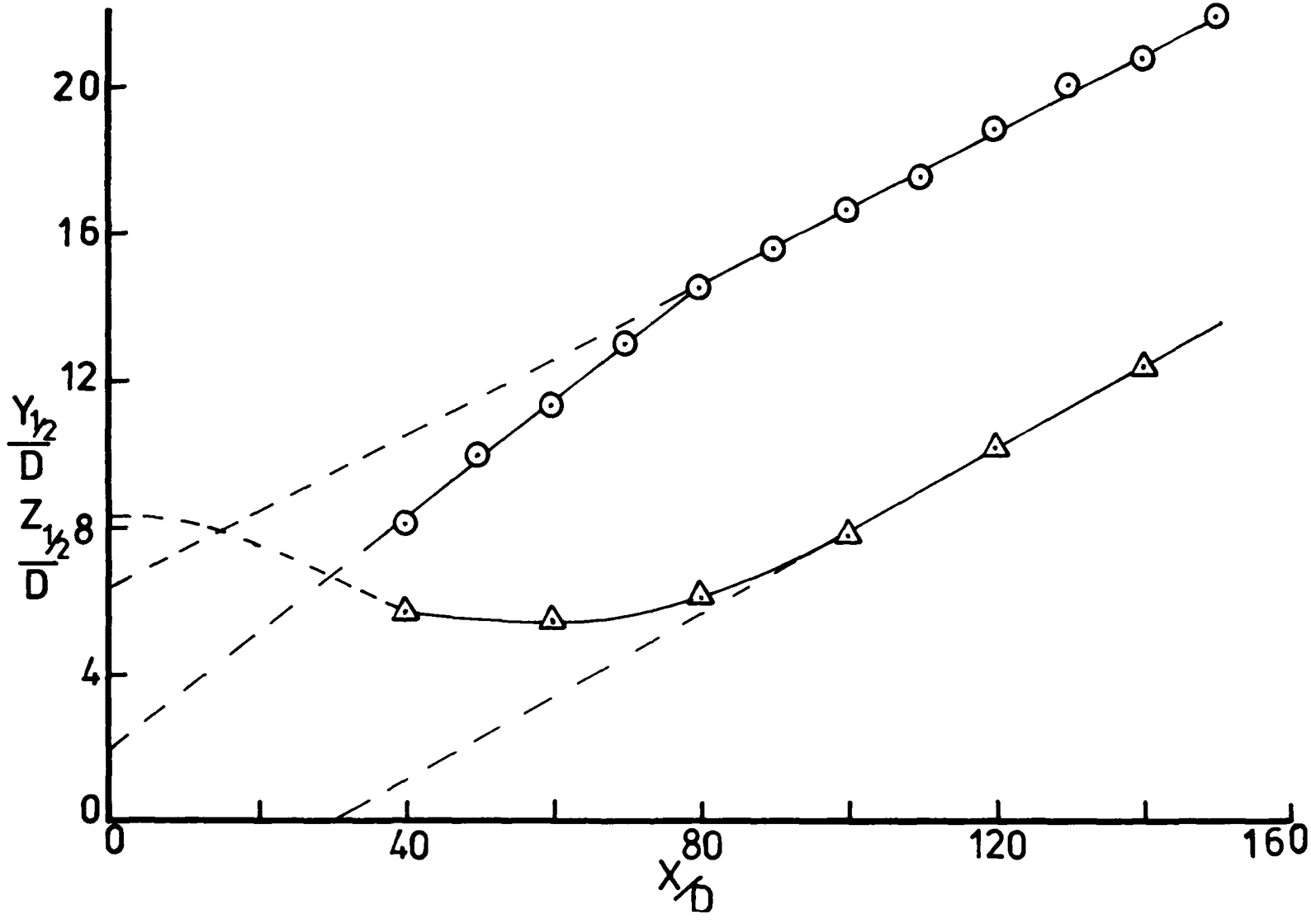

Figure 15. Growth of a rectangular jet with down stream distance.
$R = 3.8$; ⊙, $Y_{1/2}$; △, $Z_{1/2}$.

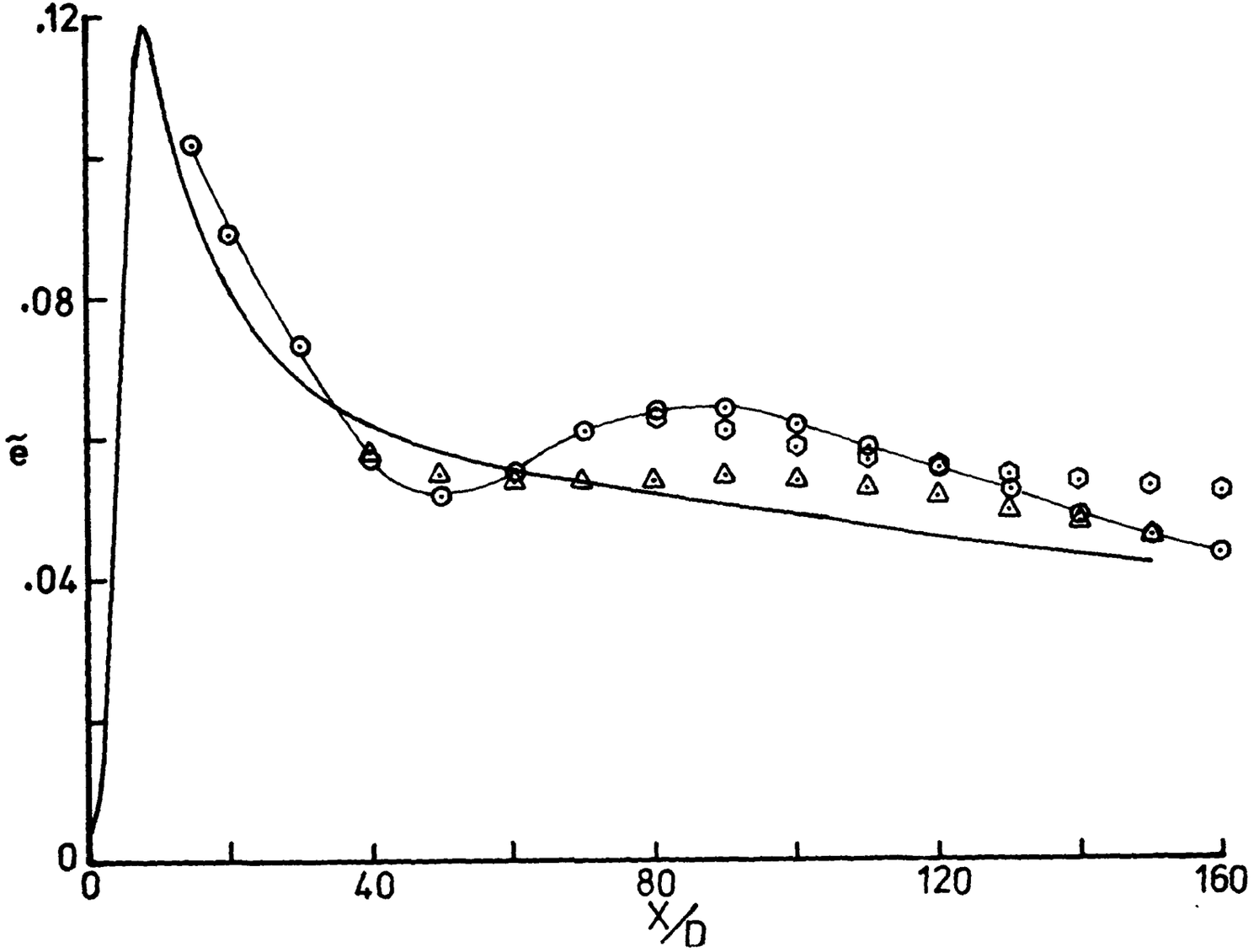

Figure 16. Variation of rms intensities along the centerline of the jet. △ , $R = 2.7$; –⊙–, $R = 3.8$; ⊡ , $R = 5.4$; ———, $M = 0.8$ (subsonic jet).

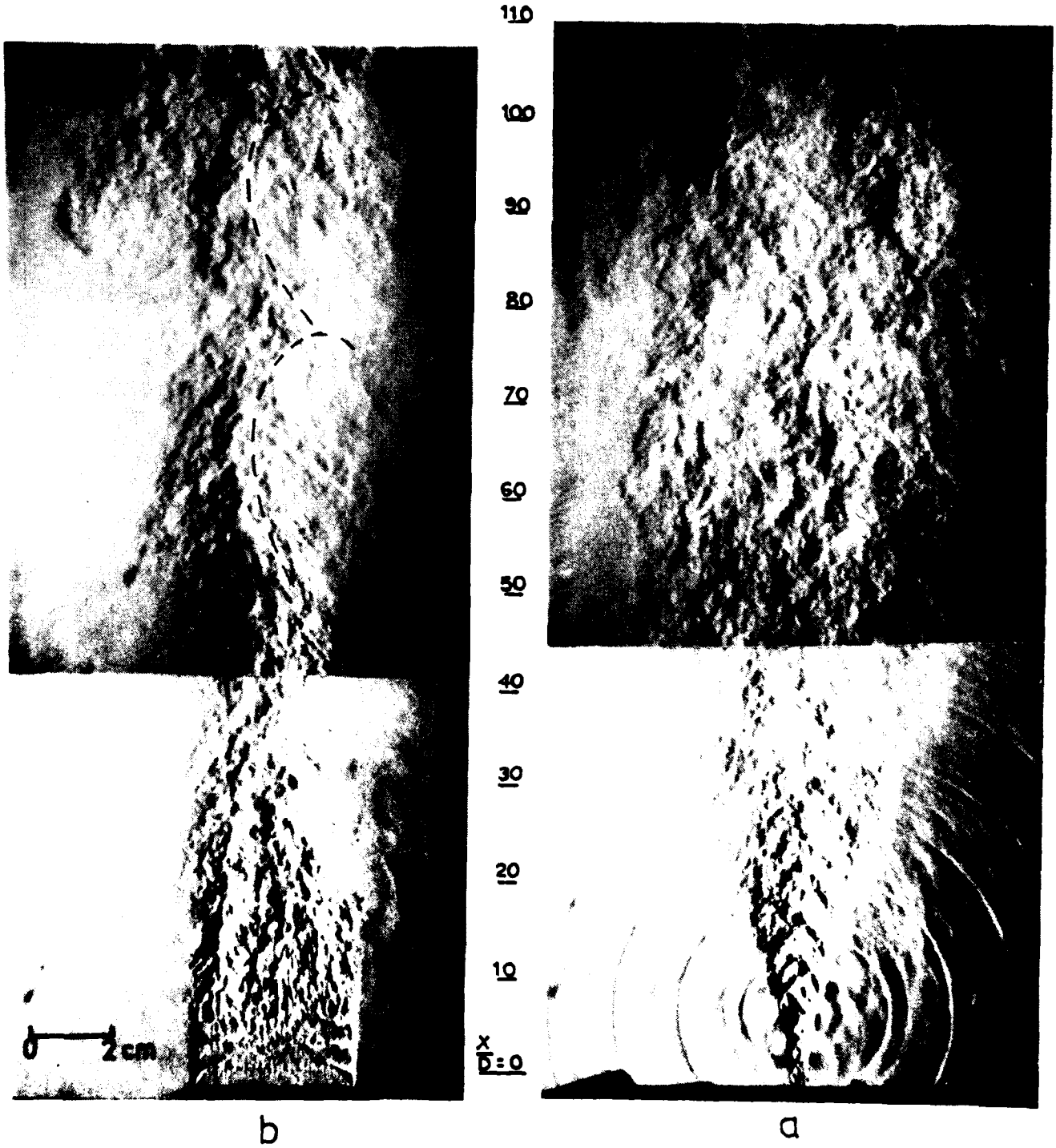

Figure 17. Schlieren pictures of the jet in both x, y and x, z planes, $R = 3.8$.

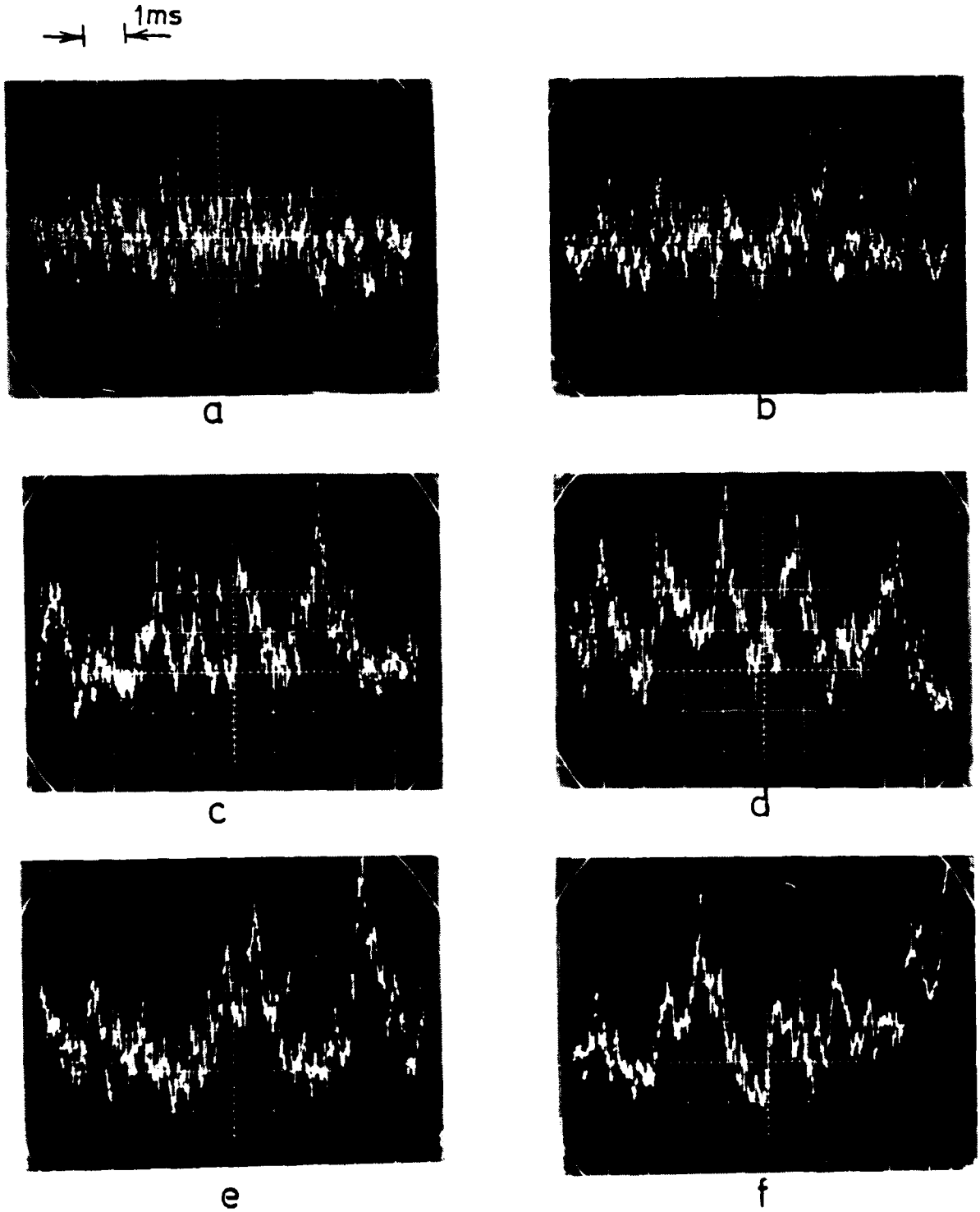

Figure 18. Oscillograms of hot wire signal along the centerline of the jet, $R = 3.8$: (a) $x/D = 40$; (b) $x/D = 60$; (c) $x/D = 80$; (d) $x/D = 100$; (e) $x/D = 120$; (f) $x/D = 140$.

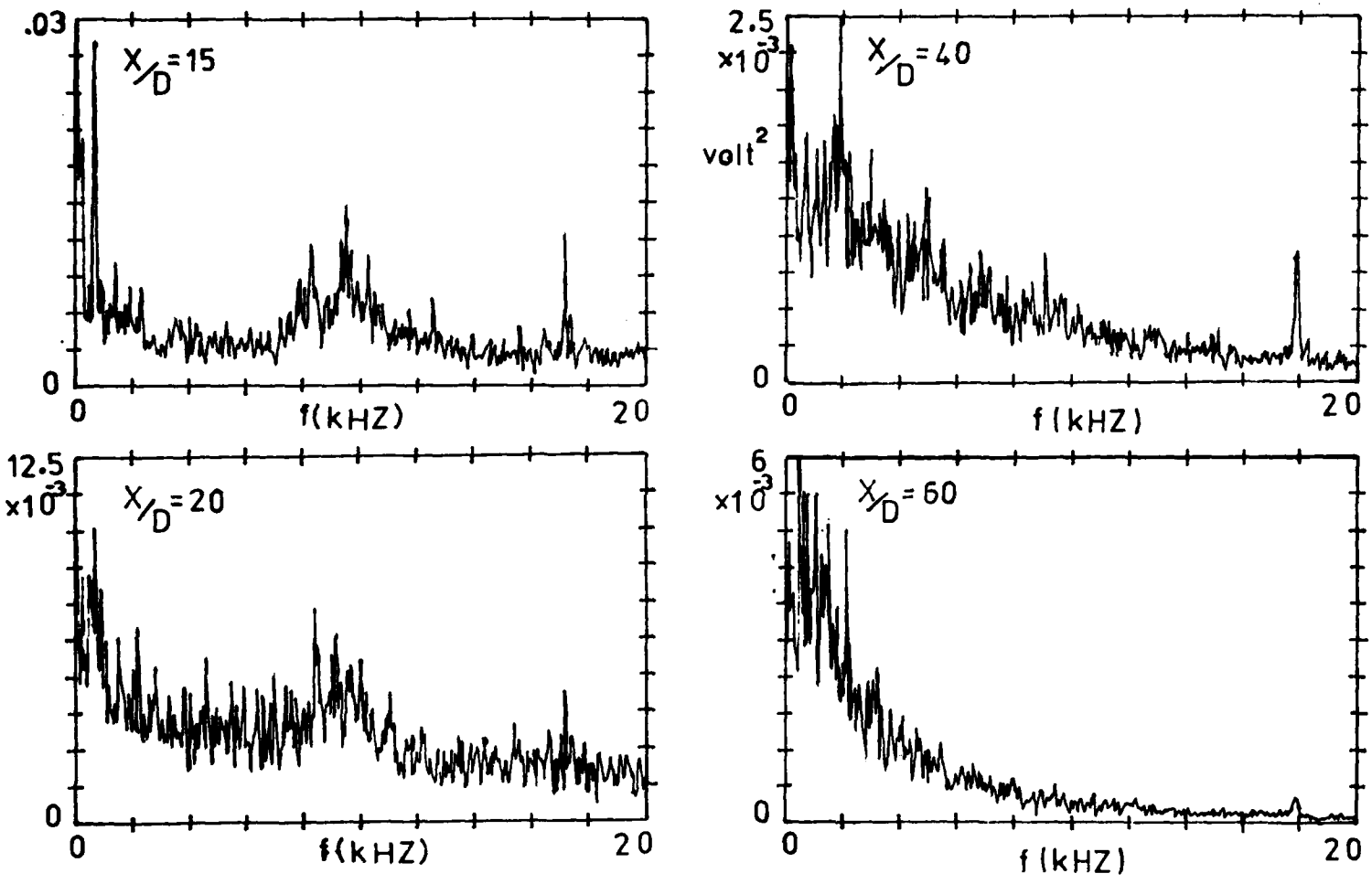

Figure 19. Continued.

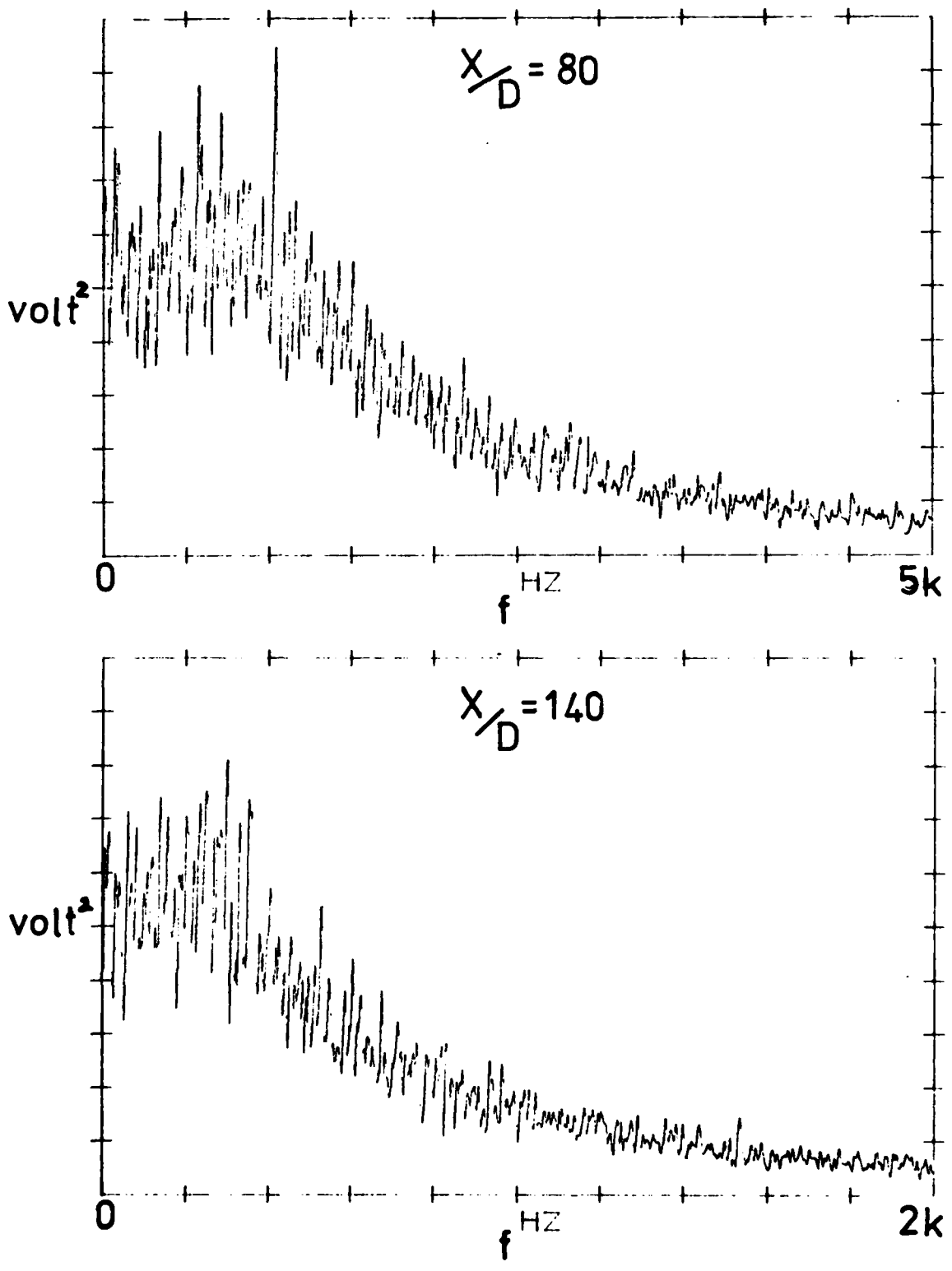

Figure 19. Specturm of hot wire or hot film voltage fluctuations along the centerline of the jet, $R = 3.8$. (a) $x/D = 15$; (b) $x/D = 20$; (c) $x/D = 40$; (d) $x/D = 60$; (e) $x/D = 80$; (f) $x/D = 140$.

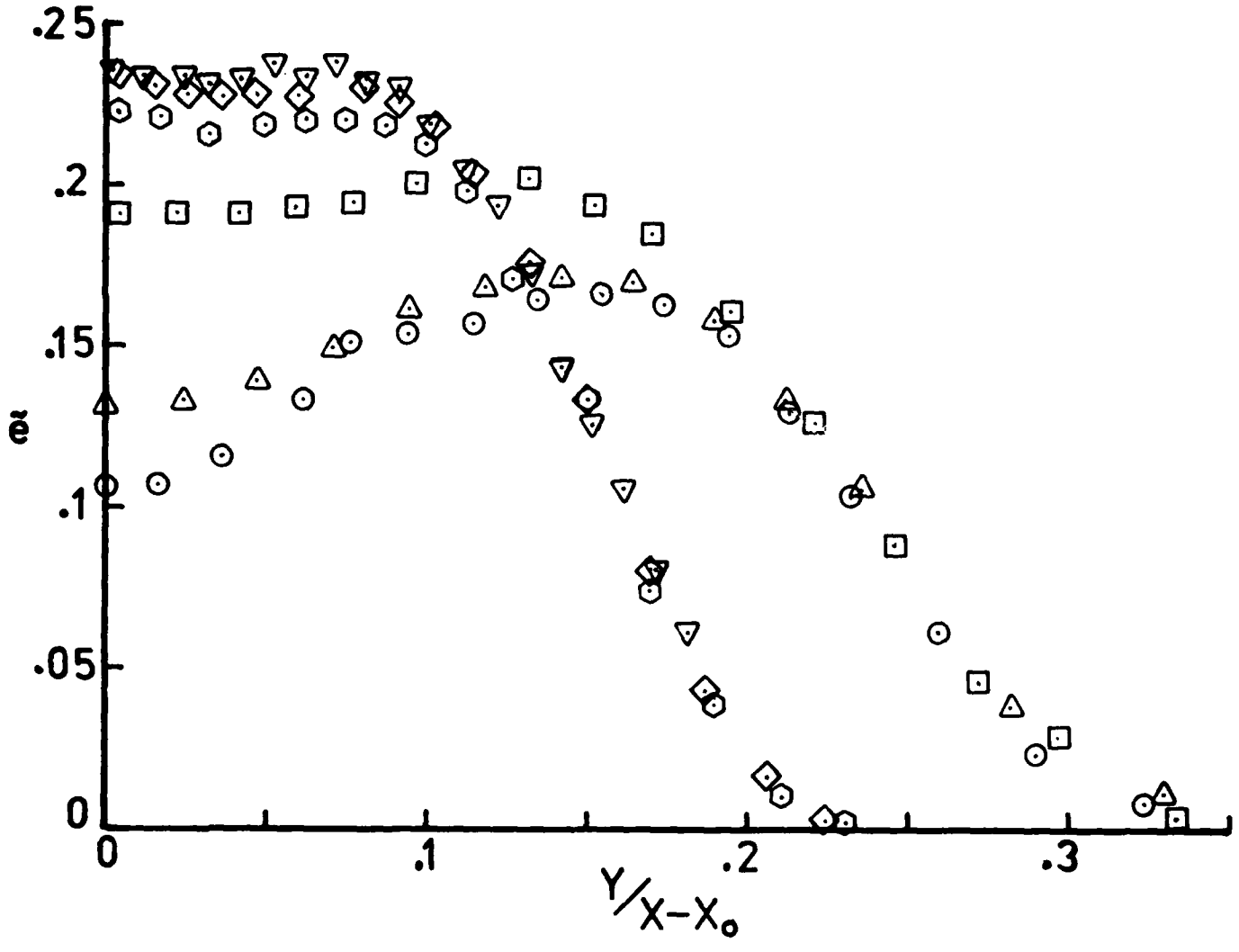

Figure 20. Distribution of rms intensities in the x, y plane, $z = 0$. $R = 3.8$, symbols as in figure 11.

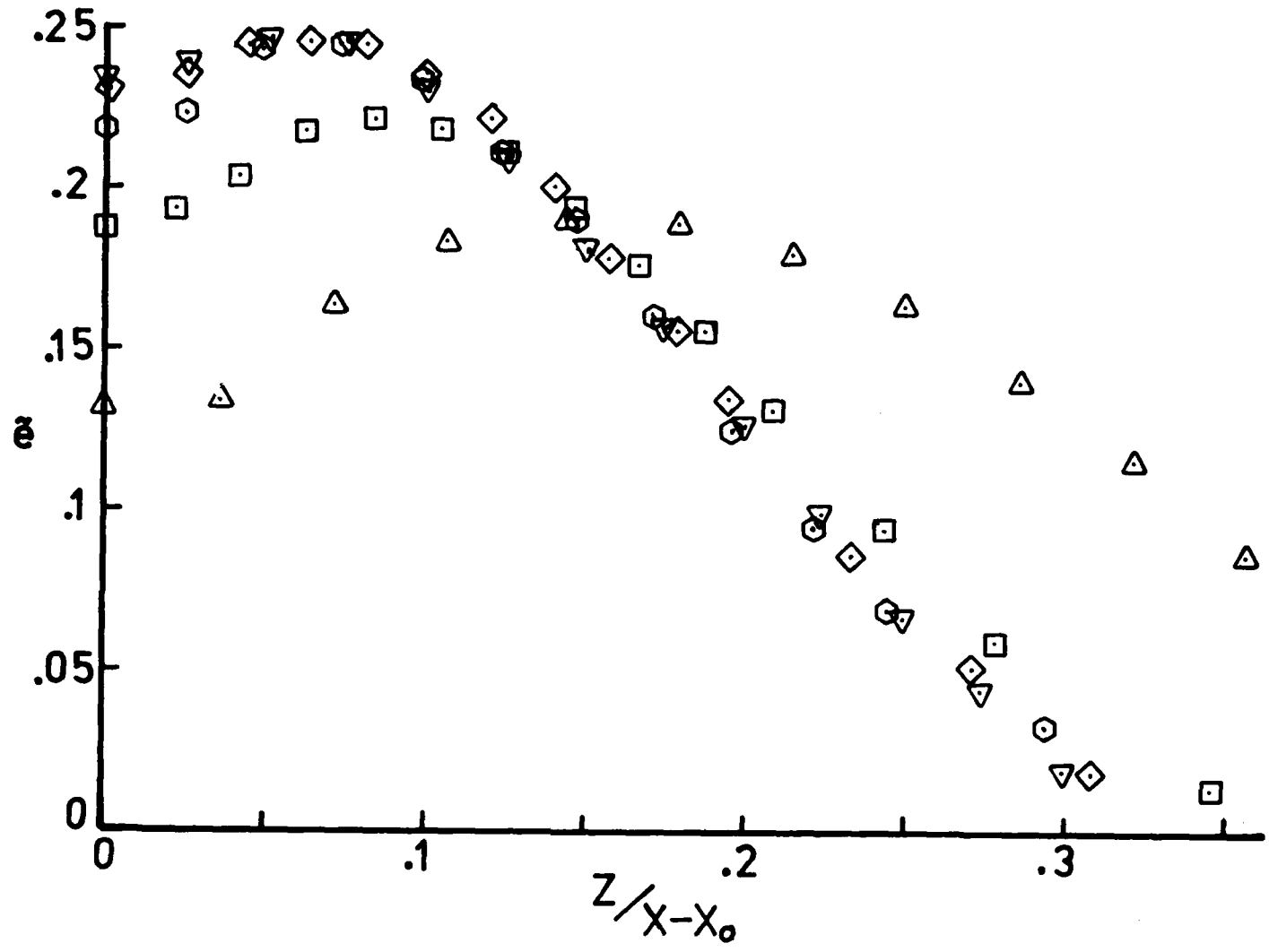

Figure 21. Distribution of rms intensities in the x, z plane, $y = 0$. $R = 3.8$, symbols as in figure 13.